Green Finance

Green Finance, 8(4): 750–780.
DOI: 10.3934/GF.2026027
Received: 25 January 2026
Revised: 28 August 2026
Accepted: 28 October 2026
Published: 10 November 2026

https://www.aimspress.com/journal/GF

Research article

Time-Varying Tail connectedness between green bonds, US tech equities, and AI/Cybersecurity ETFs: A TVP-FQVAR and machine learning approach

Mejri Sami[1,*] and Arturo Leccadito[2,3]

[1] University of Tunis El Manar, University of Management Sciences and Economics, Tunisia
[2] Department of Economics, Statistics and Finance, University of Calabria, 87036, Italy
[3] LFIN/LIDAM, UCLouvain, Voie du Roman Pays 34, Louvain la Neuve 1348, Belgium

* **Correspondence:** Email: sami.mejri@etudiant.utm.tn.

Abstract: While the convergence of sustainable finance and rapid technological innovation is changing the way portfolios are constructed, there is a lack of clear understanding of how risk moves between green bonds and high-growth technology assets, especially during periods of extreme volatility. In this study, we examined return spillovers among green bonds, major US technology equities, and AI/cybersecurity ETFs. We applied a novel Time-Varying Parameter Frequency Quantile VAR (TVP-FQVAR) framework, which decomposed connectedness across investment horizons and market states, capturing dynamics that traditional linear and static models cannot detect. We further employed SVM and XGBoost machine learning algorithms to forecast systemic connectedness using macro-financial indicators, including a novel gold-to-Bitcoin ratio. Three key findings appeared. First, overall system connectedness was high but concentrated in the short term, while long-run structural spillovers remained weak. Second, green bonds were consistently net receivers of shocks, acting as portfolio stabilizers, while technology and AI/cybersecurity ETFs were net transmitters. Third, our time-varying extension revealed that market distress (the lower return quantile) is characterized by substantial parameter instability: NVIDIA and Tesla emerged as the system's dominant net shock transmitters only once time variation was properly modeled, a dynamic concealed by static models. The strongest machine learning predictors of tail-risk connectedness were lagged VIX, inflation expectations, and the gold-to-Bitcoin ratio. These results carry direct implications for policymakers

and investors looking to adopt dynamic, regime-aware hedging strategies in the rapidly evolving sustainable-tech financial landscape.

Keywords: frequency QVAR; machine learning; green bonds; connectedness

JEL Codes: C58, C32, G11, Q56

Highlights

Innovative methodology: The TVP-FQVAR approach is developed to capture tail-risk spillovers that vary smoothly over time and across investment horizons, bypassing the biases of traditional rolling-window models.

Frequency asymmetry: Green and tech assets are consistently more connected in the short term (60–71% of total connectedness across specifications) than in the long term, where structural spillovers remain weak.

Green bonds as anchors: Despite technology-sector fluctuations, green bonds act as anchors and effective diversification tools, consistently serving as the dominant net receivers of shocks.

Hidden and reversed distress transmitters: During market distress (lower quantile), NVIDIA and Tesla emerge as the system's dominant net shock transmitters; a role static models miss for NVIDIA and get backward for Tesla, which static models instead classify as a net receiver.

Machine learning predictors: SVM and XGBoost identify the VIX, inflation expectations, and the gold-to-Bitcoin ratio as the most precise macroeconomic drivers of systemic connectedness.

1. Introduction

Global financial dynamics are being reshaped by a macroeconomic "twin transition": the convergence of the low-carbon, sustainable finance agenda with the rapid adoption of AI and digital technologies. Although these two mega-trends are often analyzed separately, their financial paths are becoming increasingly interconnected. Green bonds, a central fixed-income instrument for financing environmentally conscious projects, now coexist in investors' portfolios alongside mega-cap US technology equities, Apple, Microsoft, Amazon, NVIDIA, and Google, as well as thematic ETFs such as BOTZ and CIBR, which channel capital specifically toward AI, robotics, and cybersecurity. Both markets are also key drivers of the broader surge in AI-related investment. Assessing the dynamic interaction between these ostensibly distinct asset classes is therefore no longer solely an academic exercise; it is a practical necessity for portfolio management and systemic risk assessment.

A specific motivation for combining green bonds with AI, cybersecurity, and large-cap technology equities in a single system is the real-economy convergence of climate solutions and digital infrastructure. AI and cybersecurity are no longer peripheral to the green transition; they increasingly form part of its operational backbone, from smart-grid optimization and ESG data processing to the protection of decentralized renewable energy networks. Investor assessments of climate risk are increasingly mediated by digital tools. This mutual dependence creates a financially paradoxical

situation: Green bonds are conventionally viewed as low-volatility, defensive instruments, while AI and technology equities are high-beta, growth-oriented assets highly sensitive to interest rates and macroeconomic uncertainty. The central empirical question this raises is whether this real-economy synergy translates into financial contagion, with tech/AI equities injecting risk directly into the green bond market during periods of stress, or whether the two markets remain financially decoupled despite their operational interdependence.

The VAR-based spillover framework of Diebold and Yilmaz has been instrumental in advancing the empirical study of financial connectedness. Applied to the green-digital nexus, however, the literature leaves three distinct gaps. In the sustainable finance literature, Reboredo (2018) and Ferrer et al. (2021) have extensively documented the integration of green bonds with traditional fixed-income and energy markets, but this body of work has largely neglected the equity side of the green transition, specifically the high-growth technology and AI-related equities that supply the technological capital underpinning many climate solutions. Separately, the financial econometrics literature has established that technology-sector equity plays a substantial role in transmitting volatility across broader markets (Tunc, 2024), but these studies typically treat tech stocks as a risk source for traditional equity indices such as the S&P 500, without considering their potential spillovers into fixed-income instruments designed to finance the very projects technology increasingly enables. Methodologically, standard linear VARs cannot capture the non-linearities and asymmetries that characterize connectedness during periods of market stress; although Quantile VARs (Ando et al., 2022) and frequency-domain decompositions (Baruník and Křehlík, 2018) have advanced the toolkit considerably, their application to the green-digital asset nexus remains scarce. Finally, work on time-varying connectedness relies predominantly on rolling-window estimation, an approach well known to be sensitive to the arbitrary choice of window length and prone to artificial, discontinuous shifts around structural breaks such as the COVID-19 pandemic and the 2022–2023 monetary tightening cycle.

In this study, we pursue four research objectives to address these gaps: 1. To assess the directional spillover between green bonds, mega-cap technology stocks, and AI/cybersecurity ETFs across regions of the return distribution (favorable versus adverse market states); 2. To decompose these spillovers by investment horizon (short-term versus long-term), distinguishing transient trading dynamics from genuine structural integration; 3. To determine how individual assets' roles (net transmitter versus net receiver) evolve dynamically over time, with particular attention to the structural breaks induced by the COVID-19 crisis and the 2022–2023 monetary tightening cycle; and 4. To evaluate the effectiveness of machine learning in predicting the systemic connectedness of this asset system, using macroeconomic and market-specific predictors, including the VIX, the term-structure (yield curve) spread, inflation expectations, corporate credit spreads, and a novel gold-to-Bitcoin ratio.

The paper contributes to the literature in three main ways. First, to our knowledge, we are the first to construct a consolidated spillover network jointly linking green bonds, leading US technology equities, and thematic AI/cybersecurity ETPs, providing new empirical evidence on whether the practical convergence of climate and digital technologies is generating financial integration that could erode the diversification benefits traditionally associated with green fixed income.

Second, we extend the connectedness toolkit to a Time-Varying Parameter Frequency Quantile VAR (TVP-FQVAR), moving beyond static and rolling-window estimations. This extension enables tail-risk connectedness to evolve smoothly at daily frequency without discarding early-sample observations or imposing an arbitrarily chosen window length. Our results show that this extension is empirically consequential: It reveals substantial parameter instability during market distress (the lower

return quantile), uncovering that assets such as NVIDIA and Tesla become dominant net shock transmitters specifically once time variation is properly accounted for; a dynamic that a static model conceals entirely.

Third, beyond descriptive network mapping, we use machine learning (SVM and XGBoost) to forecast the Total Connectedness Index (TCI) out-of-sample. Feature importance plots and SHAP value decompositions are used to assess predictive accuracy and to identify which macroeconomic factors most influence systemic risk in this emerging asset system, providing portfolio managers and policymakers with actionable, data-driven signals for dynamic hedging.

The remainder of the paper is organized as follows: In Section 2, we review the related literature; in Section 3, we present the TVP-FQVAR and machine learning methodology; in Section 4, we describe the data and report descriptive statistics; In Section 5, we discuss the empirical results; and in Section 6, we conclude the study.

2. Literature review

The empirical analysis of financial connectedness is rooted in the VAR-based spillover framework of Diebold and Yilmaz, who utilize generalized forecast error variance decompositions to quantify how shocks propagate across markets and to construct total and directional connectedness indices (Diebold and Yilmaz, 2008, 2012). Building on this foundation, researchers have extended connectedness measures to capture non-linearities, asymmetries, and time-variation that become particularly pronounced during periods of market stress, highlighting the need for models that move beyond linear, mean-based relationships. In parallel, the rapid expansion of the green bond market has spurred extensive study regarding its pricing, diversification properties, and integration with conventional financial assets. While Ehlers and Packer (2017) showed that green bonds have expanded quickly as a dedicated financing instrument, and Reboredo (2018) found that they are strongly linked to sovereign and corporate bond benchmarks but only weakly related to high-yield and energy markets; recent literature offers more nuanced insights. For instance, Wei et al. (2023) demonstrated that spillovers between green bonds and energy markets are highly sensitive to the pandemic shock, intensifying significantly during the COVID-19 crisis. Similarly, Naeem et al. (2022) found that the hedging effectiveness of green bonds against clean energy and commodities varies substantially across market states, supporting the view of time-varying and state-dependent linkages. Complementing this evidence from a digital-asset perspective, Chen (2024) documented, via a DCC-GJR-GARCH connectedness and wavelet coherence framework, that Bitcoin exhibits only weak positive correlation with green bond assets and therefore is an ineffective hedge for green bond exposure, further underscoring green bonds' relative insulation from the broader digital-asset ecosystem examined in this study.

Concurrently, the rise of mega-cap US technology firms, such as Amazon, Tesla, Alphabet/Google, Microsoft, and Nvidia, alongside thematic ETFs focused on robotics, artificial intelligence, and cybersecurity (e.g., BOTZ and CIBR), has re-shaped equity markets. These high-beta, growth-oriented assets exhibit strong sensitivity to interest-rate expectations and macro-financial uncertainty, possessing considerable potential to generate and transmit shocks across sectors. This systemic influence is corroborated by Tu et al. (2024) who documented that high-tech sectors like Fintech exhibit dynamic and bidirectional connectedness with traditional stock markets, often acting as net transmitters of volatility during turbulent periods. However, the joint behavior of green bonds

and high-growth technology assets is under-explored, particularly in a framework that distinguishes downside, median, and upside market states and separates short- and long-horizon spillovers.

To address the limitations of linear, time-domain VARs in such settings, quantile regression (Koenker and Bassett, 1978) and its multivariate extensions enable the conditional dependence structure of returns to be modeled across the distribution. Moreover, frequency-domain connectedness methods, such as those of Baruník and Křehlík (2018), decompose spillovers into short-, medium-, and long-run components associated with heterogeneous investment horizons. The value of this frequency decomposition is well illustrated in the literature, with researchers like Konstantakis et al, (2025) employing these techniques to disentangle the time-scale dynamics of spillovers between alternative assets and commodities. Combining these two perspectives, Chatziantoniou et al. (2022) developed a quantile time–frequency price connectedness framework and showed that green bonds, green equity, and clean-energy indices exhibit quantile- and horizon-dependent spillovers that are highly sensitive to global shocks. These findings motivate the use of a Frequency Quantile VAR (FQVAR) approach to study the connectedness between green bonds, US high-tech stocks, and AI/cybersecurity ETFs in our study.

Finally, macro-financial variables such as the VIX, corporate credit spreads (the ICE BofA US Corporate Index Option-Adjusted Spread), the term spread between 10-year and 2-year US Treasuries, and measures of inflation expectations play a central role in explaining time-variation in systemic risk and connectedness, as they capture shifts in uncertainty, funding conditions, and monetary policy (Estrella and Mishkin, 1998; Gilchrist and Zakrajšek, 2012). In parallel, a growing body of researchers applies machine-learning models such as support vector machines, gradient-boosted trees (XGBoost), and neural networks to financial forecasting and systemic-risk measurement, with applications ranging from volatility and return prediction to tail-risk and spillover modeling (Hoang et al., 2023; Rundo et al., 2019). These models are particularly well suited to capturing complex, non-linear interactions between connectedness measures and macro-financial drivers. They can be paired with explainable-AI tools to identify which variables, such as volatility indices, yield-curve slopes, credit spreads, or the gold/Bitcoin ratio, contribute most to forecasted changes in spillovers, thereby complementing the structural insights obtained from the FQVAR framework.

To sum up, while the literature has made significant progress in describing financial connectedness, there remains an important gap between sustainable finance and the digital economy that is being driven by AI. Researchers have failed to acknowledge the symbiotic real-economy relationship between green bonds and technology equities. Additionally, methodological dependence on linear, mean-based models, or static quantile frameworks makes it difficult to determine the spillover effects across investment horizons in highly volatile market environments. The utilization of arbitrary rolling-window estimations to capture time-variation leaves findings exposed to parameter instability during structural breaks, such as the COVID-19 pandemic and the aggressive monetary tightening cycle. In this study, we utilize a two-fold econometric model to address these complex gaps. Our initial step is to implement a fresh Time-Varying Parameter Frequency Quantile VAR (TVP-FQVAR). This approach removes the limitations of earlier studies by decomposing spillovers in the frequency domain (short- vs. long-term investment horizons) and quantile domain while enabling network topologies to evolve smoothly without discarding sample observations. Recognizing that simply identifying spillovers is not enough for practical risk management, we integrate machine learning algorithms like SVM and XGBoost to forecast systemic connectedness and isolate macroeconomic drivers that dictate its evolution.

3. Methodology

3.1. The Frequency Quantile VAR (FQVAR) Methodology

The Frequency Quantile Vector Autoregression (FQVAR) approach of Chatziantoniou et al. (2022) enables measuring dynamic connectedness and directional spillovers among financial markets, combining information from the quantile (tail) and frequency (investment horizon) domains.

Let $\mathbf{y}_t$ be an $N \times 1$ vector of endogenous return series. The FQVAR is based on the Quantile Vector Autoregression (QVAR) model, which extends traditional VAR analysis to conditional quantiles:

$$Q_{\mathbf{y_t}}(\tau \mid \mathcal{F}_{t-1}) = \boldsymbol{\mu}(\tau) + \sum_{i=1}^{p} \boldsymbol{\Phi}_i(\tau)\mathbf{y}_{t-i} + \boldsymbol{\xi}_t(\tau) \tag{1}$$

where $\tau \in (0,1)$ is the quantile of interest, $Q_{\mathbf{y_t}}(\tau \mid \mathcal{F}_{t-1})$ is the vector of conditional quantiles given past information, $\boldsymbol{\mu}(\tau)$ and $\boldsymbol{\Phi}_i(\tau)$ are quantile-specific intercepts and coefficient matrices, p is the lag order, and $\boldsymbol{\xi}_t(\tau)$ is the quantile innovation vector.

Using Wold's theorem, Chatziantoniou et al. (2022) used the following Quantile Vector Moving Average (QVMA) to represent the QVAR model:

$$\mathbf{y}_t(\tau) = \sum_{j=0}^{\infty} \boldsymbol{\Psi}_j(\tau)\boldsymbol{\xi}_{t-j}(\tau) \tag{2}$$

and derive the Generalized Forecast Error Variance Decomposition (GFEVD):

$$\theta_{jk}(H;\tau) = \frac{\sum_{h=0}^{H-1}\left[e_j'\boldsymbol{\Psi}_h(\tau)\Sigma(\tau)e_k\right]^2}{\Sigma_{kk}(\tau)\sum_{h=0}^{H-1}\left[e_j'\boldsymbol{\Psi}_h(\tau)\Sigma(\tau)\boldsymbol{\Psi}_h(\tau)e_j\right]} \tag{3}$$

where H is the forecast horizon, $\boldsymbol{\Psi}_h(\tau)$ is the impulse response at quantile τ, $\Sigma(\tau)$ is the covariance matrix at quantile τ, and e_j is a selection vector for variable j with one in position j and zero in all the remaining positions.

Connectedness measures are based on the normalized θ_{jk}:

$$\tilde{\theta}_{jk}(H;\tau) = \frac{\theta_{jk}(H;\tau)}{\sum_{k=1}^{N}\theta_{jk}(H;\tau)} \tag{4}$$

The Total Connectedness Index (TCI), quantifying the average spillover effects for the network is defined as:

$$TCI(H;\tau) = \frac{1}{N}\sum_{j\neq k}\tilde{\theta}_{jk}(H;\tau) \tag{5}$$

The Directional Connectedness To and From others are defined respectively as

$$TO_j(H;\tau) = \sum_{k\neq j}\tilde{\theta}_{kj}(H;\tau) \tag{6}$$

and as

$$FROM_j(H;\tau) = \sum_{k \neq j} \tilde{\theta}_{jk}(H;\tau) \tag{7}$$

Finally, the Net Directional Connectedness is defined as:

$$NET_j(H;\tau) = TO_j(H;\tau) - FROM_j(H;\tau) \tag{8}$$

The authors then transform the time-domain GFEVD using the spectral decomposition:

$$d_{jk}(\omega;\tau) = \frac{\left|\sum_{h=0}^{\infty} e_j' \boldsymbol{\Psi}(\tau)\left(\mathrm{e}^{-\mathrm{i}\omega h}\right)\Sigma(\tau)e_k\right|^2}{\Sigma_{kk}(\tau)\sum_{h=0}^{\infty} e_j' \boldsymbol{\Psi}(\tau)(\mathrm{e}^{-\mathrm{i}\omega h})\Sigma(\tau)\boldsymbol{\Psi}(\tau)(\mathrm{e}^{\mathrm{i}\omega h})e_j} \tag{9}$$

Here, ω indexes frequency, $\boldsymbol{\Psi}(\tau)(\mathrm{e}^{-\mathrm{i}\omega h}) = \sum_{h=0}^{\infty} \mathrm{e}^{-\mathrm{i}\omega h}\boldsymbol{\Psi}_h(\tau)$, and $\boldsymbol{\Psi}(\tau)(\mathrm{e}^{\mathrm{i}\omega h}) = \sum_{h=0}^{\infty} \mathrm{e}^{\mathrm{i}\omega h}\boldsymbol{\Psi}_h(\tau)$. Short-term ($\omega \in [\omega_1, \omega_2]$) and long-term ($\omega > \omega_2$) connectedness indices can hence be computed by integrating $d_{jk}(\omega;\tau)$ over appropriate frequency bands.

3.1.1. A Time-Varying Parameter Extension: The TVP-FQVAR

The FQVAR in Section 3.1 delivers a single, full-sample estimate of $\boldsymbol{\Phi}_i(\tau)$ and $\Sigma(\tau)$ and therefore a static picture of tail connectedness across the sample period. To trace how connectedness evolves through time, the literature has traditionally re-estimated the QVAR on rolling windows of fixed length, w. This approach is well known to be sensitive to the arbitrary choice of w, to discard the first w observations, and to produce estimates that react abruptly to outliers entering or leaving the window (Antonakakis et al., 2020). Given that our sample spans the COVID-19 period and the subsequent rate-hike cycle, this concern is particularly relevant: Connectedness parameters plausibly shifted across these distinct regimes, and a single static estimate, or one based on an arbitrarily chosen rolling window, may not adequately capture this instability. We therefore complement the rolling-window results with a genuinely time-varying alternative that extends the Time-Varying Parameter VAR (TVP-VAR) connectedness approach of Antonakakis et al. (2020), built on the logic of Koop and Korobilis (2014), to the conditional-quantile setting of Section 3.1. We refer to the resulting framework as the Time-Varying Parameter Frequency Quantile VAR (TVP-FQVAR).

For a given quantile $\tau \in (0,1)$ and for each equation $j = 1, \ldots, N$, the time-t coefficients $\widehat{\boldsymbol{\mu}}_{j,t}(\tau)$ and $\widehat{\boldsymbol{\Phi}}_{j,i,t}(\tau)$ are obtained from an exponentially discounted quantile regression,

$$\left(\widehat{\boldsymbol{\mu}}_{j,t}(\tau),\ \widehat{\boldsymbol{\Phi}}_{j,1,t}(\tau), \ldots, \widehat{\boldsymbol{\Phi}}_{j,p,t}(\tau)\right) = \underset{\mu_j,\, \boldsymbol{\Phi}_{j,1},\ldots,\boldsymbol{\Phi}_{j,p}}{\operatorname{argmin}} \sum_{s=1}^{t} \kappa_1^{t-s}\ \rho_\tau\left(y_{j,s} - \mu_j - \sum_{i=1}^{p} \boldsymbol{\Phi}_{j,i}\ \mathbf{y}_{s-i}\right)$$

where $\rho_\tau(u) = u(\tau - \mathbb{1}\{u < 0\})$ and $\kappa_1 \in (0,1]$ is a coefficient forgetting factor, playing the same role as in the TVP-VAR of Antonakakis et al. (2020): it controls the effective memory of the recursion, with observations $t - s$ periods in the past down-weighted geometrically at rate κ_1^{t-s}.

Stacking $\widehat{\boldsymbol{\Phi}}_{j,i,t}(\tau)$ over $i = 1, \ldots, p$ and $j = 1, \ldots, N$ yields the time-t coefficient matrices $\boldsymbol{\Phi}_{i,t}(\tau)$, and the corresponding quantile residuals $\boldsymbol{\xi}_t(\tau)$ are used to update the residual covariance matrix through an exponentially weighted moving average with a second forgetting factor $\kappa_2 \in (0,1]$,

$$\Sigma_t(\tau) = \kappa_2\, \Sigma_{t-1}(\tau) + (1 - \kappa_2)\boldsymbol{\xi}_t(\tau)\boldsymbol{\xi}_t(\tau)'$$

again mirroring the covariance state equation of the TVP-VAR of Antonakakis et al. (2020). The recursion is initialized with a static QVAR fit, $\widehat{\boldsymbol{\Phi}}_i(\tau)$ and $\hat{\Sigma}(\tau) = \widehat{\mathrm{Var}}(\boldsymbol{\xi})$, over a burn-in sample, after which $\{\boldsymbol{\Phi}_{i,t}(\tau),\ \Sigma_t(\tau)\}$ evolve recursively for every subsequent t.

As $\kappa_1 \to 1$, the discounted loss converges to the (expanding-window) full-sample QVAR loss of Section 3.1, so the static FQVAR is nested as the limiting case $\kappa_1 = \kappa_2 = 1$. Lower values of κ_1 shorten the effective window and make $\boldsymbol{\Phi}_{i,t}(\tau)$ more responsive to recent observations, at the cost of higher estimation variance, exactly the bias-variance trade-off governed by the window length w in the rolling-window QVAR, but resolved smoothly rather than through a hard cut-off.

Given the sequence of time-t QVAR estimates $\{\boldsymbol{\Phi}_{i,t}(\tau), \Sigma_t(\tau)\}_{t=1}^{T}$, the frequency-domain decomposition of Baruník and Křehlík (2018) described in Section 3.1 is applied period-by-period rather than once on the full sample. Each $\boldsymbol{\Phi}_{i,t}(\tau)$ is used to recover the time-t QVMA representation $\boldsymbol{\Psi}_{h,t}(\tau)$, from which the time-varying generalized FEVD, spectral density, and connectedness measures follow directly from equations (3)-(9) of Section 3.1 with an added time subscript:

$$d_{jk,t}(\omega;\tau) = \frac{\left|\sum_{h=0}^{\infty} e_j'\boldsymbol{\Psi}_t(\tau)\left(\mathrm{e}^{-i\omega h}\right)\Sigma_t(\tau)e_k\right|^2}{\Sigma_{kk,t}(\tau)\sum_{h=0}^{\infty} e_j'\boldsymbol{\Psi}_t(\tau)(\mathrm{e}^{-i\omega h})\,\Sigma_t(\tau)\boldsymbol{\Psi}_t(\tau)(e^{i\omega h})e_j}$$

Integrating $d_{jk,t}(\omega;\tau)$ over the short-term ($\omega \in [\omega_1, \omega_2]$) and long-term ($\omega > \omega_2$) frequency bands, exactly as in Section 3.1, produces the time-varying total, directional, and net connectedness measures $TCI_t(H;\tau)$, $TO_{j,t}(H;\tau)$, $FROM_{j,t}(H;\tau)$, and $NET_{j,t}(H;\tau)$, disaggregated by investment horizon. Unlike the rolling-window QVAR, the TVP-FQVAR produces a connectedness estimate for every t in the sample (net of the burn-in period) without imposing a fixed window length, thereby avoiding the arbitrary choice of w and the associated loss of initial observations. The average of these time-varying measures across the full sample, together with their evolution across the COVID-19 and rate-hike sub-periods, is reported in Section 5 as a robustness check on the parameter stability of the static and rolling-window results.

Following the calibration typically used in the TVP-VAR connectedness literature (Antonakakis et al., 2020; Koop and Korobilis, 2014), we set $\kappa_1 = \kappa_2 = 0.99$ as the baseline and assess the sensitivity of the results to this choice as a robustness check.

3.2. Machine learning models

We use machine learning algorithms to predict spillover dynamics and to identify the most influential macro-financial determinants contributing to systemic connectedness. Two core models,Support Vector Machines (SVM) and Extreme Gradient Boosting (XGBoost), are implemented and compared in terms of predictive accuracy and interpretability.

3.2.1. Support Vector Machines (SVM)

The SVM model is adopted using a radial basis function (RBF) kernel to handle non-linearities inherent in financial spillovers. This kernel maps the input feature space, comprising macroeconomic indicators such as the VIX, the gold/Bitcoin ratio, credit spread differentials, and the Treasury yield spread, into a higher dimension where linear separability becomes feasible. SVM seeks a function that deviates from the observed targets by no more than a specified threshold ε while minimizing model complexity. The resulting optimization problem is

$$\min_{\mathbf{w},b,\xi,\xi^*} \frac{1}{2}\|\mathbf{w}\|^2 + C\sum_{i=1}^{n}(\xi_i + \xi_i^*)$$

subject to

$$\begin{gathered} y_i - \mathbf{w}'\phi(\boldsymbol{x}_i) - b \leq \varepsilon + \xi_i \\ \mathbf{w}'\phi(\boldsymbol{x}_i) + b - y_i \leq \varepsilon + \xi_i^* \\ \xi_i, \xi_i^* \geq 0 \end{gathered}$$

where y_i denotes the i-th observation for the vector of input variables, n represents the number of observations, $\mathbf{w}$ and b parameterize the regression function, C is a regularization parameter, $\phi(\cdot)$ maps the inputs $\boldsymbol{x}_i$ into a higher-dimensional space, and ξ_i, ξ_i^* are the errors outside the ε −tolerance margin. The RBF kernel, which has the following form:

$$K(\boldsymbol{x}_i, \boldsymbol{x}_j) = e^{-\beta\|\boldsymbol{x}_i - \boldsymbol{x}_j\|^2}, \beta > 0$$

is related to the feature mapping function $\phi(\cdot)$ as follows: $K(\boldsymbol{x}_i, \boldsymbol{x}_j) = \phi(\boldsymbol{x}_i)'\phi(\boldsymbol{x}_j)$. The hyperparameters are selected through grid search cross-validation to minimize the Root Mean Square Error (RMSE).

3.2.2. Extreme Gradient Boosting (XGBoost)

Extreme Gradient Boosting (XGBoost) is another ML technique based on a sequence of decision trees, i.e., a supervised machine learning algorithm that uses a tree-like model to make predictions. With XGBoost, each new tree attempts to correct the residual errors of the combined previous trees. The method starts with an initial prediction, often a simple average of the target variable, and, after the first tree is built, it calculates the residuals. The subsequent trees are trained to predict these residuals, not the original target variable. The final forecast is a weighted sum of the predictions from all the individual trees (ensemble prediction).

The model prediction for an input $\boldsymbol{x}_i$ with K trees is expressed as

$$\hat{y}_i = \sum_{k=1}^{K} f_k(\boldsymbol{x}_i),$$

where f_k represents the function learned by the k-th regression tree. The objective function at iteration t is defined as the sum of a loss function and a regularization term:

$$\text{Obj}^{(t)}(\theta) = \sum_{i=1}^{n} l\left(y_i, \hat{y}_i^{(t)}\right) + \sum_{k=1}^{t} \Omega(f_k)$$

where θ denotes all parameters of the model, and $l\left(y_i, \hat{y}_i^{(t)}\right)$ represents the loss function that measures, for the i-th observation, the difference between the actual value y_i and the predicted value $\hat{y}_i^{(t)}$. The regularization term $\Omega(f_k)$ penalizes the complexity of the tree f_k and it is typically defined as:

$$\Omega(f_k) = \gamma T + \lambda\frac{1}{2}\|\mathbf{w}\|^2$$

where T is the number of leaves in the tree, $\mathbf{w}$ is the vector of scores in each leaf, γ is the minimum loss reduction required to justify a further split (the per-leaf complexity penalty), and λ is the L2 regularization coefficient applied to the leaf weights.

To identify the optimal new tree f_t that minimizes the objective function, XGBoost uses a gradient descent algorithm to minimize the loss function:

$$\text{Obj}^{(t)}(\theta) \approx \sum_{i=1}^{n} \left[g_i f_t(x_i) + \frac{1}{2} h_i f_t^2(x_i) \right] + \Omega(f_t)$$

where $g_i = \partial_{\hat{y}_i} l\left(y_i, \hat{y}_i^{(t-1)}\right)$ is the gradient and $h_i = \partial_{\hat{y}_i}^2 l\left(y_i, \hat{y}_i^{(t-1)}\right)$ is the Hessian matrix.

3.2.3. Model evaluation

To identify the most influential determinants of systemic connectedness, interpretability tools are employed in addition to forecasting metrics like RMSE and the coefficient of determination (R^2). For XGBoost, we report Gain-based feature importance, which is the model's native measure of a predictor's average contribution to loss reduction across all splits. For SVM, given the absence of a native importance measure for kernel-based models, we report a univariate filter-based importance, computed as the R^2 of a LOESS smoother relating each predictor individually to the connectedness outcome. To supplement these importance measures, SHAP value decomposition is applied to isolate individual predictor effects on model output. Based on Shapley values from cooperative game theory, SHAP values quantify each feature's marginal contribution to deviations from the model's expected output. Observations with high SHAP magnitudes correspond to strong predictors. SHAP summary and dependence plots facilitate transparent attribution of predictive variance in both ML frameworks.

3.2.4. Hyperparameter Tuning and Cross-Validation

Hyperparameters for the SVM and XGBoost models are selected through a walk-forward cross-validation scheme, rather than a single in-sample fit. Specifically, each model is repeatedly trained on a rolling window of 500 observations and evaluated on the single subsequent, out-of-sample observation (one-step-ahead forecasting); the window is then advanced by one observation and the process repeated across the full sample, so that no hyperparameter combination is ever evaluated on data used in its own estimation.

For each rolling fold, hyperparameters are selected from a pre-specified grid: for the SVM, a 3×3 grid over the regularization parameter $C \in \{0.1, 1, 10\}$ and the RBF kernel bandwidth $\sigma \in \{0.01, 0.1, 1\}$ (9 combinations); for XGBoost, a 128-point grid spanning the number of boosting rounds $\{50, 100\}$, maximum tree depth $\{2, 4\}$, learning rate $\{0.1, 0.3\}$, minimum loss reduction $\gamma \in \{0, 0.1\}$, column subsampling ratio $\{0.7, 1\}$, minimum child weight $\{1, 2\}$, and row subsampling ratio $\{0.7, 1\}$. For a given feature set, the hyperparameter combination that minimizes the average out-of-sample RMSE across all rolling folds is selected, and the forecasting performance reported in Section 5 (RMSE and out-of-sample R^2) is computed from the corresponding pooled out-of-fold predictions at that combination, that is, exclusively from predictions on observations never used to either estimate the model or select its hyperparameters. Because this evaluation is genuinely out-of-sample, unlike in-

sample R^2, it is not mechanically non-decreasing in the number of predictors: Additional features improve forecasting performance only insofar as their relationship with the dependent variable is stable enough to generalize beyond the training window on which the model is estimated, and can otherwise increase the risk of overfitting within a given window and reduce out-of-sample accuracy, as discussed further in Section 5.

4. Data description

Table 1 reports the descriptive statistics for the data used in the paper. The explanatory variables we use are the gold/Bitcoin ratio (RATIO), the 10-year minus 2-year Treasury yield spread (T10Y2Y), the five-year inflation expectation (T5YIFR), the VIX index (VIXCLS), and the ICE BofA Option-Adjusted Spread (BAMLC0A0CM)[1].

Table 1. Descriptive statistics.

Panel A: returns × 100.

	GREEN.BONDS	BOTZ	CIBR	NVDA	MSFT	AAPL	AMZN	TSLA	GOOG
Mean	−0.003	0.027	0.062	0.232	0.081	0.074	0.060	0.169	0.066
Median	0.000e+00	0.090	0.160	0.316	0.096	0.114	0.071	0.166	0.198
Maximum	2.272	11.986	9.695	21.809	13.293	14.262	12.695	20.449	9.499
Minimum	−2.410	−13.246	−10.571	−20.398	−15.945	−13.771	−15.140	−23.652	−11.767
St. Dev	0.460	1.862	1.696	3.464	1.937	2.069	2.299	4.280	2.076
Skewness	−0.012	−0.261	−0.466	0.046	−0.164	0.023	−0.073	−0.056	−0.223
Kurtosis	5.945	9.557	7.427	6.741	10.317	9.134	7.079	6.221	6.557
Jarque-Bera	487.519	2428.066	1149.268	786.858	3010.017	2112.095	935.679	583.757	721.971
P-value	0.000e+00	0.000e+00	0.000e+00	0.000e+00	0.000e+00	0.000e+00	0.000e+00	0.000e+00	0.000e+00
N. Observations	1341	1341	1341	1341	1341	1341	1341	1341	1341

Panel B. explanatory variables.

	T5YIFR	VIXCLS	BAMLC0A0CM	T10Y2Y	RATIO
Mean	2.151	21.544	1.208	0.188	0.060
Median	2.240	19.740	1.100	0.200	0.059
Maximum	2.670	82.690	4.010	1.590	0.137
Minimum	0.860	11.860	0.770	−1.080	0.009
St. Dev	0.267	8.176	0.383	0.657	0.031
Skewness	−1.557	2.507	2.621	0.214	0.185
Kurtosis	5.104	13.965	14.343	2.085	2.075
Jarque-Bera	792.045	8151.424	8755.453	56.705	55.240
P-value	0.000e+00	0.000e+00	0.000e+00	4.861e-13	1.011e-12
N. Observations	1341	1341	1341	1341	1341

[1] BAMLC0A0CM measures the average yield spread of US dollar-denominated investment-grade corporate bonds over a duration-matched US Treasury curve, after adjusting for the value of embedded options in the bonds (such as call provisions).

Figure 1 and Figure 2 provide the time-series plots of returns (x 100) of the tech stocks or ETFs and of the explanatory variables, respectively.

Based on the provided data, a detailed analysis of the descriptive statistics and time-series visualizations for the tech assets and explanatory variables is provided. Table 1 is divided into two panels, providing statistical summaries for 1,341 observations.

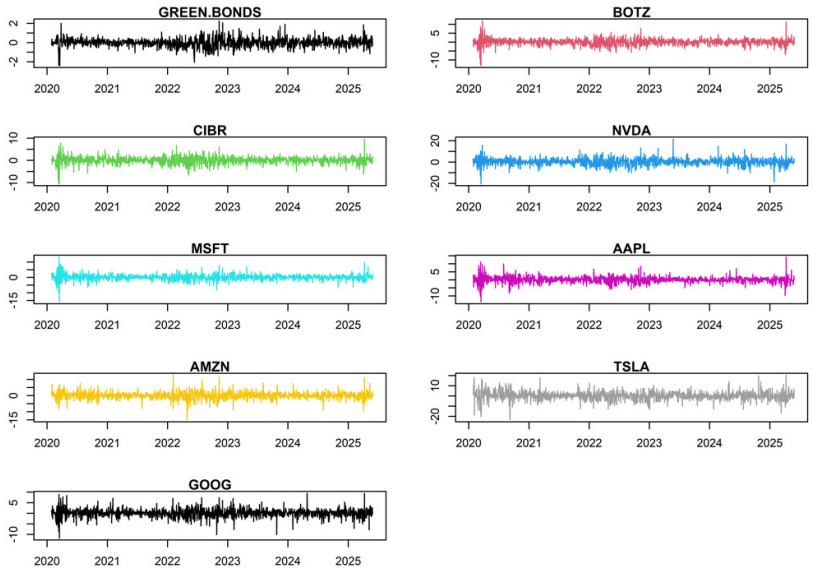


Figure 1. Time Series Plots, returns × 100.

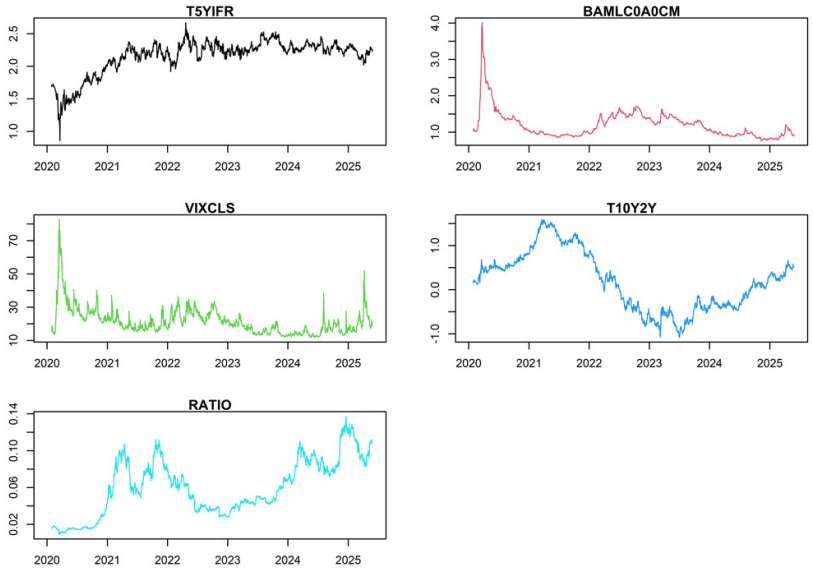


Figure 2. Time Series Plots, explanatory variables.

This panel summarizes the performance of Green Bonds, tech ETFs (BOTZ, CIBR), and major tech stocks (NVDA, MSFT, AAPL, AMZN, TSLA, GOOG). NVDA shows the highest mean return at 0.232, followed by TSLA at 0.169. GREEN.BONDS is the only asset with a negative mean return (-0.003). TSLA is the most volatile asset with a standard deviation of 4.280 and the largest range between its maximum (20.449) and minimum (−23.652) returns. NVDA also shows high volatility (3.464). Green bonds are the most stable series with a standard deviation of only 0.46. Most assets exhibit negative skewness (e.g., CIBR at -0.466), indicating a higher frequency of small gains and occasional large losses. NVDA and AAPL are slight outliers with positive skewness. All assets show high kurtosis (all > 3.0), particularly MSFT (10.317) and BOTZ (9.557), suggesting fat tails or a high probability of extreme return events. The Jarque-Bera test results, combined with P-values of 0.000, indicate that the returns for all assets are not normally distributed.

The second panel details the macro-financial indicators used as predictors. The VIXCLS (volatility index) has a high mean of 21.544 and reaches a staggering maximum of 82.690, reflecting periods of extreme market stress. T5YIFR (Inflation expectations) averages 2.151%. T10Y2Y (Yield curve) shows a mean of 0.188, but its minimum of -1.080 indicates a significant period of yield curve inversion. Like the asset returns, high Jarque-Bera scores and P-values near zero confirm that these variables do not follow a normal distribution.

The plots in Figure 1 visualize the daily fluctuations summarized in Table 1.

All assets, particularly the high-growth stocks like NVDA and TSLA, show volatility clustering where periods of high volatility are grouped together, especially around early 2020 (the COVID-19 market shock) and throughout 2022. The GREEN BONDS plot is visibly tighter than the individual stocks, confirming its lower risk profile observed in the descriptive statistics.

Figure 2 tracks the movement of market drivers over time. A massive spike is visible in early 2020 for VIXCLS, corresponding with the onset of the pandemic. The blue plot for the yield curve shows a downward trend starting in 2021, dropping below the zero line (inversion) through 2023 and 2024, which is often viewed as a recession signal. The BAMLC0A0CM (Credit Spreads) plot shows a sharp peak in early 2020, indicating a temporary spike in credit risk that stabilizes.

5. Results

In this section, we unveil the static connectedness obtained by considering the FQVAR models between Green Bonds, the US high-tech stocks, and artificial intelligence and cybersecurity indices. ML models are subsequently used to explain the resulting connectedness indices.

5.1. Results of static connectedness

Tables 2 and 3 report the results for the lower (5%) and upper quantile (95%), respectively. Each table presents the Total, short-term (ranging from 1 to 5 days, $\omega \in (\pi/5, \pi)$), and long-term (from 6 to infinite days, $\omega \in (0, \pi/5]$) connectedness measures.

Table 2. Connectedness Measures, Lower Quantile (5%).

	GREEN.BONDS	BOTZ	CIBR	NVDA	MSFT	AAPL	AMZN	TSLA	GOOG	FROM
Total										
GREEN.BONDS	17.18	11.08	10.74	10.00	10.38	10.17	10.23	10.20	10.02	82.82
BOTZ	9.16	13.56	11.74	11.54	11.13	10.69	11.05	10.46	10.67	86.44
CIBR	8.92	11.78	13.97	10.97	11.60	10.65	11.19	10.39	10.54	86.03
NVDA	8.64	11.76	11.11	14.56	11.40	10.50	11.02	10.24	10.76	85.44
MSFT	8.47	11.10	11.45	10.94	14.28	11.07	11.51	9.79	11.39	85.72
AAPL	8.95	10.97	10.96	10.45	11.62	14.36	11.06	10.32	11.30	85.64
AMZN	8.48	11.12	11.28	10.76	11.65	10.65	14.64	10.01	11.40	85.36
TSLA	9.05	11.10	11.11	10.75	10.79	10.58	10.61	15.67	10.34	84.33
GOOG	8.70	10.95	10.94	10.64	11.74	11.02	11.48	9.78	14.75	85.25
TO	70.38	89.86	89.33	86.05	90.31	85.33	88.15	81.19	86.42	767.03
Inc.Own	87.56	103.43	103.30	100.61	104.59	99.68	102.79	96.87	101.17	cTCI/TCI
Net	−12.44	3.43	3.30	0.61	4.59	−0.32	2.79	−3.13	1.17	95.88/85.23
NPDC	0.00	7.00	6.00	2.00	8.00	3.00	5.00	1.00	4.00	
Short										
GREEN.BONDS	12.71	7.79	7.37	6.97	7.17	7.21	7.36	7.00	7.14	58.01
BOTZ	6.73	10.09	8.50	8.35	8.06	7.87	8.15	7.55	8.02	63.24
CIBR	6.21	8.38	9.70	7.58	7.95	7.49	7.95	7.10	7.59	60.23
NVDA	6.59	9.11	8.36	11.10	8.55	8.04	8.46	7.75	8.41	65.28
MSFT	6.41	8.53	8.43	8.27	10.77	8.44	8.78	7.23	8.75	64.85
AAPL	6.93	8.60	8.29	8.16	8.91	11.10	8.59	7.86	8.93	66.26
AMZN	6.87	8.98	8.83	8.57	9.15	8.66	11.80	7.91	9.28	68.25
TSLA	7.33	8.99	8.76	8.70	8.52	8.58	8.59	12.55	8.42	67.88
GOOG	7.04	8.74	8.53	8.40	9.17	8.81	9.18	7.66	11.92	67.53
TO	54.10	69.12	67.09	64.98	67.48	65.10	67.07	60.06	66.54	581.54
Inc.Own	66.81	79.20	76.79	76.08	78.24	76.21	78.87	72.60	78.46	cTCI/TCI
Net	−3.91	5.88	6.86	−0.29	2.63	−1.16	−1.18	−7.83	−0.99	72.69/64.62
NPDC	1.00	7.00	8.00	4.00	6.00	3.00	2.00	0.00	5.00	
Long										
GREEN.BONDS	4.47	3.29	3.37	3.03	3.21	2.96	2.87	3.20	2.88	24.81
BOTZ	2.43	3.48	3.24	3.19	3.07	2.81	2.90	2.91	2.65	23.20
CIBR	2.72	3.40	4.27	3.39	3.66	3.16	3.23	3.29	2.95	25.80
NVDA	2.05	2.65	2.76	3.46	2.85	2.45	2.56	2.49	2.35	20.16
MSFT	2.07	2.57	3.01	2.66	3.52	2.62	2.73	2.56	2.64	20.86
AAPL	2.03	2.37	2.67	2.30	2.71	3.25	2.47	2.47	2.37	19.38
AMZN	1.61	2.15	2.45	2.19	2.50	1.99	2.83	2.10	2.12	17.12
TSLA	1.72	2.11	2.35	2.05	2.27	2.00	2.02	3.13	1.92	16.44
GOOG	1.66	2.21	2.41	2.25	2.57	2.21	2.30	2.12	2.83	17.72
TO	16.28	20.75	22.24	21.07	22.83	20.22	21.08	21.14	19.88	185.49
Inc.Own	20.75	24.22	26.51	24.53	26.35	23.48	23.91	24.26	22.71	cTCI/TCI
Net	−8.53	−2.45	−3.56	0.90	1.97	0.84	3.96	4.69	2.17	23.19/20.61
NPDC	0.00	2.00	1.00	3.00	5.00	4.00	7.00	8.00	6.00	

The study of static connectedness exhibits a significant trend, especially for the lower quantile of 5%. TCI (85.23%) is overwhelmingly driven by the short-term component (64.62%), which is approximately three times the magnitude of the long-term component (20.61%). Despite this sharp contrast, it seems likely that market integration is more rapid. Furthermore, US stocks exhibit uniform spillover effects from green bonds of about 8 and 9 per cent, suggesting an even spread of shocks. In the same way, spillovers among US stocks oscillate at similar levels, seldom exceeding 14%, and suggest a weak shock transmission. The correlation between connectedness and temporal dynamics is worth examining, given that short and long-term connections diminish across frequency bands; amplitudes drop to less than 4% in the long run. The evidence for weak shock transmission and market integration is supported by this discovery. However, the results also show that US high-tech stocks and green bonds provide a means of diversification against downside risk during adverse market conditions. These assets offer investors a chance to reduce losses and benefit from the relatively weak market

integration. Especially during market stress periods, this provides compelling evidence that diversification is crucial in maintaining balance and managing portfolios strategically.

Table 3. Connectedness Measures, Upper Quantile (95%).

	GREEN.BONDS	BOTZ	CIBR	NVDA	MSFT	AAPL	AMZN	TSLA	GOOG	FROM
Total										
GREEN.BONDS	17.14	11.09	10.47	10.38	10.29	10.34	10.01	9.98	10.29	82.86
BOTZ	8.73	14.35	11.88	11.76	11.10	10.67	10.68	9.99	10.84	85.65
CIBR	8.63	11.97	14.67	11.15	11.34	10.65	10.78	10.29	10.52	85.33
NVDA	8.47	11.98	11.44	14.91	11.26	10.53	10.59	10.12	10.70	85.09
MSFT	8.01	11.16	11.36	11.17	14.71	11.23	11.22	9.62	11.52	85.29
AAPL	8.75	11.03	11.03	10.68	11.54	15.11	10.68	10.22	10.98	84.89
AMZN	8.21	11.14	11.24	10.92	11.62	10.80	14.98	9.68	11.41	85.02
TSLA	8.83	11.12	11.20	11.06	10.57	10.86	10.35	15.56	10.44	84.44
GOOG	8.33	11.08	10.69	10.80	11.98	10.78	11.22	9.58	15.54	84.46
TO	67.96	90.56	89.31	87.93	89.70	85.87	85.52	79.47	86.70	763.03
Inc.Own	85.10	104.92	103.99	102.83	104.41	100.98	100.50	95.04	102.24	cTCI/TCI
Net	−14.90	4.92	3.99	2.83	4.41	0.98	0.50	−4.96	2.24	95.38/84.78
NPDC	0.00	8.00	7.00	5.00	6.00	3.00	2.00	1.00	4.00	
Short										
GREEN.BONDS	12.33	7.71	7.46	7.32	6.97	7.19	6.89	7.08	7.10	57.73
BOTZ	7.25	11.87	9.97	9.82	9.11	8.89	8.75	8.43	9.00	71.22
CIBR	7.22	9.95	12.31	9.44	9.38	8.92	9.08	8.75	8.92	71.67
NVDA	7.28	10.33	9.95	12.93	9.59	9.14	9.11	8.70	9.27	73.38
MSFT	6.63	9.36	9.58	9.40	12.17	9.45	9.35	8.16	9.65	71.56
AAPL	7.39	9.35	9.33	9.09	9.56	12.80	8.98	8.76	9.27	71.73
AMZN	6.36	8.90	8.98	8.77	9.12	8.67	11.89	7.79	9.04	67.65
TSLA	7.22	9.03	9.12	9.10	8.52	8.95	8.56	12.66	8.60	69.09
GOOG	6.06	8.17	7.92	8.01	8.92	8.22	8.29	7.09	11.56	62.68
TO	55.41	72.80	72.31	70.94	71.17	69.43	69.01	64.77	70.86	616.70
Inc.Own	67.74	84.67	84.62	83.88	83.34	82.22	80.90	77.43	82.43	cTCI/TCI
Net	−2.32	1.58	0.64	−2.43	−0.39	−2.30	1.36	−4.33	8.19	77.09/68.52
NPDC	2.00	6.00	6.00	2.00	4.00	2.00	6.00	0.00	8.00	
Long										
GREEN.BONDS	4.81	3.38	3.01	3.06	3.32	3.15	3.11	2.90	3.19	25.13
BOTZ	1.48	2.48	1.91	1.95	1.99	1.77	1.93	1.56	1.84	14.42
CIBR	1.41	2.01	2.36	1.71	1.96	1.73	1.70	1.53	1.60	13.66
NVDA	1.19	1.64	1.50	1.97	1.67	1.39	1.48	1.42	1.42	11.72
MSFT	1.39	1.80	1.78	1.77	2.54	1.78	1.87	1.47	1.87	13.73
AAPL	1.36	1.68	1.70	1.58	1.98	2.31	1.70	1.46	1.70	13.16
AMZN	1.85	2.24	2.25	2.15	2.49	2.13	3.09	1.89	2.38	17.38
TSLA	1.61	2.10	2.08	1.97	2.05	1.92	1.79	2.90	1.84	15.34
GOOG	2.27	2.91	2.77	2.79	3.06	2.56	2.93	2.48	3.98	21.78
TO	12.55	17.76	17.00	16.98	18.53	16.44	16.52	14.71	15.84	146.33
Inc.Own	17.36	20.25	19.36	18.95	21.07	18.75	19.61	17.61	19.81	cTCI/TCI
Net	−12.58	3.34	3.34	5.26	4.80	3.28	−0.86	−0.64	−5.95	18.29/16.26
NPDC	0.00	5.00	4.00	8.00	7.00	6.00	2.00	3.00	1.00	

A pattern of heightened market integration in the short term is evident at the upper quantile (τ =95%), where several pairwise short-term linkages reach 10% to 15%, indicating stocks' vulnerability to macroeconomic shocks. However, green bonds are a resilient diversification mechanism, as their total connectedness remains below 9%. Investors are best protected against short-term market turbulence by holding green bonds, as these figures and the stark disparity in asset classes highlight. This evidence underscores the need for investors to prioritize risk-based returns over more low-key assets during periods of market optimism. Even though short-term interdependencies dictate most market behavior, the long-run connection remains elusive, rarely exceeding 3%, even during periods of great integration. A smaller linkage indicates structural differences in asset return patterns over time, which gives investors a strategic edge. Portfolios can benefit from the asymmetry between

short-term volatility and long-lasting stability, which enables green bonds to be more muted in response to extended systemic shocks. These findings not only confirm the feasibility of robust diversification but also advocate for rebalancing measures that prioritize green assets as anchors of strength during expansionary phases.

5.2. Results of dynamic connectedness

Tables 4 and 5 report the average connectedness measures using the newly proposed TVP-FQVAR method.

Table 4. Average Connectedness Measures, Lower Quantile (5%).

	GREEN.BONDS	BOTZ	CIBR	NVDA	MSFT	AAPL	AMZN	TSLA	GOOG	FROM
Total										
GREEN.BONDS	16.59	10.54	11.17	11.14	10.46	9.41	9.64	11.71	9.34	83.41
BOTZ	9.08	12.97	12.25	12.62	11.26	9.92	10.29	11.77	9.83	87.03
CIBR	9.00	11.40	14.13	12.32	11.34	9.66	10.66	11.96	9.52	85.87
NVDA	8.62	11.31	11.82	15.09	11.31	9.75	10.42	11.93	9.74	84.91
MSFT	8.64	10.81	11.75	12.13	13.83	10.29	10.66	11.44	10.46	86.17
AAPL	8.91	10.69	11.34	11.91	11.53	12.98	10.39	11.89	10.35	87.02
AMZN	8.50	10.52	11.65	11.99	11.34	9.81	13.89	12.00	10.30	86.11
TSLA	9.07	10.32	11.41	11.98	10.61	9.74	10.42	16.95	9.51	83.05
GOOG	8.91	10.55	11.22	11.79	11.76	10.31	10.84	11.57	13.04	86.96
TO	70.74	86.14	92.62	95.88	89.62	78.88	83.31	94.27	79.06	770.51
Inc.Own	87.33	99.11	106.75	110.97	103.45	91.87	97.21	111.21	92.11	cTCI/TCI
Net	−12.67	−0.89	6.75	10.97	3.45	−8.13	−2.79	11.21	−7.89	96.31/85.61
NPDC	0.00	4.00	6.00	8.00	5.00	1.00	3.00	7.00	2.00	
Short										
GREEN.BONDS	11.33	6.79	6.83	6.70	6.69	6.36	6.25	6.86	6.21	52.68
BOTZ	6.25	9.50	8.38	8.50	8.06	7.45	7.29	7.66	7.38	60.98
CIBR	5.80	7.83	9.24	7.74	7.62	6.87	7.20	7.32	6.75	57.13
NVDA	6.07	8.55	8.33	10.74	8.35	7.57	7.67	7.97	7.56	62.09
MSFT	5.98	8.04	8.12	8.27	10.23	7.86	7.73	7.46	7.97	61.44
AAPL	6.30	8.11	8.00	8.25	8.60	10.11	7.62	7.99	8.03	62.89
AMZN	6.15	8.04	8.31	8.44	8.48	7.84	10.66	8.23	8.18	63.67
TSLA	6.33	7.66	7.89	8.19	7.67	7.50	7.62	11.85	7.25	60.12
GOOG	6.74	8.30	8.32	8.52	9.08	8.34	8.46	8.13	10.59	65.88
TO	49.63	63.32	64.18	64.61	64.55	59.80	59.84	61.61	59.33	546.87
Inc.Own	60.97	72.82	73.42	75.35	74.78	69.91	70.49	73.45	69.92	cTCI/TCI
Net	−3.05	2.34	7.05	2.52	3.11	−3.09	−3.83	1.49	−6.55	68.36/60.76
NPDC	1.00	6.00	8.00	5.00	7.00	3.00	2.00	4.00	0.00	
Long										
GREEN.BONDS	5.26	3.75	4.34	4.43	3.77	3.05	3.39	4.86	3.14	30.73
BOTZ	2.83	3.48	3.87	4.12	3.20	2.47	3.00	4.11	2.45	26.05
CIBR	3.20	3.58	4.89	4.57	3.72	2.79	3.46	4.64	2.77	28.74
NVDA	2.55	2.76	3.49	4.35	2.96	2.18	2.74	3.96	2.18	22.82
MSFT	2.65	2.76	3.63	3.86	3.61	2.42	2.92	3.98	2.50	24.73
AAPL	2.61	2.58	3.34	3.66	2.94	2.87	2.77	3.91	2.32	24.13
AMZN	2.34	2.48	3.34	3.56	2.86	1.96	3.24	3.76	2.12	22.43
TSLA	2.74	2.66	3.52	3.79	2.94	2.24	2.80	5.10	2.25	22.94
GOOG	2.17	2.25	2.90	3.28	2.68	1.97	2.38	3.44	2.46	21.07
TO	21.10	22.82	28.44	31.27	25.07	19.08	23.47	32.66	19.73	223.64
Inc.Own	26.36	26.29	33.33	35.62	28.68	21.95	26.71	37.76	22.19	cTCI/TCI
Net	−9.63	−3.23	−0.30	8.45	0.34	−5.05	1.04	9.73	−1.35	27.95/24.85
NPDC	0.00	2.00	4.00	7.00	5.00	1.00	6.00	8.00	3.00	

Table 5. Average Connectedness Measures, Upper Quantile (95%).

	GREEN.BONDS	BOTZ	CIBR	NVDA	MSFT	AAPL	AMZN	TSLA	GOOG	FROM
Total										
GREEN.BONDS	17.14	11.14	10.14	10.09	10.28	10.05	10.12	10.52	10.53	82.86
BOTZ	8.67	14.11	11.72	11.70	11.34	10.75	10.52	10.16	11.03	85.89
CIBR	8.48	12.20	13.93	11.19	11.31	10.80	10.81	10.42	10.85	86.07
NVDA	8.20	12.31	11.35	14.40	11.64	10.73	10.61	10.01	10.75	85.60
MSFT	7.96	11.51	11.14	11.20	14.23	11.54	11.14	9.87	11.41	85.77
AAPL	8.32	11.37	11.01	10.80	11.98	14.67	10.74	10.10	11.01	85.33
AMZN	8.55	11.09	10.90	10.78	11.45	10.68	14.86	10.29	11.39	85.14
TSLA	8.76	11.12	11.04	10.89	10.76	10.69	10.55	15.45	10.74	84.55
GOOG	8.39	11.31	10.75	10.72	11.87	11.05	11.11	9.99	14.81	85.19
TO	67.33	92.06	88.05	87.37	90.63	86.29	85.61	81.37	87.69	766.40
Inc.Own	84.47	106.17	101.98	101.77	104.86	100.96	100.47	96.82	102.50	cTCI/TCI
Net	−15.53	6.17	1.98	1.77	4.86	0.96	0.47	−3.18	2.50	95.80/85.16
NPDC	0.00	8.00	5.00	4.00	7.00	3.00	3.00	1.00	5.00	
Short										
GREEN.BONDS	12.51	7.97	7.33	7.23	7.28	7.16	7.19	7.63	7.59	59.38
BOTZ	7.36	11.98	10.05	9.94	9.66	9.20	8.84	8.74	9.38	73.17
CIBR	7.43	10.61	12.04	9.76	9.84	9.43	9.38	9.13	9.51	75.10
NVDA	7.22	10.92	10.09	12.69	10.27	9.51	9.29	8.78	9.50	75.59
MSFT	6.86	10.10	9.79	9.76	12.36	10.12	9.65	8.65	9.94	74.86
AAPL	7.14	9.88	9.50	9.32	10.29	12.61	9.19	8.72	9.42	73.46
AMZN	6.81	9.17	8.97	8.89	9.35	8.80	12.07	8.37	9.26	69.62
TSLA	6.99	8.83	8.85	8.69	8.59	8.59	8.49	12.28	8.64	67.68
GOOG	6.73	9.19	8.71	8.68	9.65	9.08	8.91	8.03	11.83	68.98
TO	56.55	76.67	73.30	72.26	74.93	71.89	70.94	68.05	73.24	637.83
Inc.Own	69.06	88.65	85.34	84.95	87.29	84.49	83.01	80.33	85.07	cTCI/TCI
Net	−2.82	3.50	−1.80	−3.33	0.07	−1.57	1.32	0.37	4.26	79.73/70.87
NPDC	1.00	7.00	2.00	1.00	4.00	2.00	6.00	5.00	8.00	
Long										
GREEN.BONDS	4.63	3.17	2.80	2.86	3.00	2.88	2.94	2.90	2.93	23.48
BOTZ	1.31	2.13	1.66	1.76	1.68	1.55	1.69	1.42	1.64	12.72
CIBR	1.05	1.59	1.89	1.43	1.46	1.38	1.43	1.29	1.34	10.97
NVDA	0.98	1.39	1.26	1.71	1.36	1.22	1.32	1.23	1.24	10.01
MSFT	1.10	1.41	1.35	1.44	1.87	1.42	1.49	1.23	1.47	10.91
AAPL	1.17	1.49	1.51	1.48	1.69	2.06	1.55	1.38	1.59	11.87
AMZN	1.74	1.92	1.93	1.89	2.10	1.88	2.79	1.92	2.13	15.52
TSLA	1.76	2.30	2.19	2.20	2.17	2.10	2.05	3.17	2.10	16.87
GOOG	1.66	2.13	2.04	2.04	2.22	1.97	2.20	1.95	2.98	16.21
TO	10.78	15.39	14.75	15.11	15.70	14.40	14.67	13.32	14.45	128.57
Inc.Own	15.41	17.52	16.64	16.82	17.58	16.46	17.46	16.49	17.43	cTCI/TCI
Net	−12.71	2.67	3.78	5.10	4.80	2.53	−0.85	−3.55	−1.76	16.07/14.29
NPDC	0.00	4.00	6.00	8.00	7.00	5.00	3.00	1.00	2.00	

Comparing the time-varying parameter estimates of Tables 4 and 5 with the static estimates of Tables 2 and 3 provides an informative check on the parameter stability of the connectedness system across the sample, which spans the COVID-19 period and the subsequent rate-hike cycle. At the aggregate level, the correspondence is close: The average Total TCI implied by the TVP-FQVAR is 85.61% at the lower quantile and 85.16% at the upper quantile, essentially unchanged from the static estimates of 85.23% and 84.78%, respectively. This indicates that the overall degree of systemic connectedness reported in Section 5.1 is not an artifact of assuming constant parameters over the full sample and is robust to enable the underlying VAR coefficients to evolve recursively through time.

Beneath this aggregate stability, however, the frequency decomposition reveals a more nuanced picture. At the lower quantile ($\tau = 5\%$), the time-varying estimates attribute less of the total connectedness to the short-term component (60.76% versus 64.62% under the static model) and correspondingly more to the long-term component (24.85% versus 20.61%). At the upper quantile ($\tau = 95\%$), the pattern reverses: The time-varying short-term share rises slightly (70.87% versus 68.52%)

while the long-term share falls (14.29% versus 16.26%). This suggests that, once genuine time variation is enabled, tail connectedness during market distress ($\tau = 5\%$) carries a somewhat more persistent, longer-horizon component than the static model implies, whereas connectedness during calmer upper-quantile conditions remains concentrated, if anything more so, in the short-term band.

The most notable divergence between the static and time-varying estimates, however, concerns the directional roles of individual assets rather than the aggregate connectedness level. At the upper quantile, the net transmitter/receiver ranking is remarkably stable across the two specifications: Green bonds remain the dominant net receiver (net −14.90 static versus −15.53 time-varying), BOTZ and MSFT remain the leading net transmitters (4.92/4.41 static versus 6.17/4.86 time-varying), and the ordering of the remaining assets is essentially preserved. At the lower quantile, by contrast, the two specifications diverge sharply. Under the static model, NVDA and TSLA are close to net-neutral or mild net receivers (net 0.61 and −3.13, respectively), while BOTZ, CIBR, and MSFT are the leading net transmitters. Under the time-varying model, this ordering is substantially reshuffled: NVDA and TSLA emerge as the two strongest net transmitters in the system (net 10.97 and 11.21), while AAPL, AMZN, and GOOG–modest transmitters or near-neutral under the static model–become net receivers (net −8.13, −2.79, and −7.89, respectively).

This asymmetry is an informative finding. It indicates that the parameter instability one might expect from a sample spanning the COVID-19 shock and the subsequent tightening cycle is concentrated in the lower-tail (distress) regime, where the identity of net shock transmitters shifts materially once time variation is accounted for, rather than being uniformly distributed across the return distribution. Upper-quantile connectedness, associated with calmer or positively trending market conditions, appears considerably more stable to this same test. From a practical standpoint, this implies that static, full-sample estimates of which assets transmit shocks during market stress should be interpreted with caution, even though the overall magnitude of stress-period connectedness they report is not misleading. We view this as a substantive contribution of the TVP-FQVAR extension, directly responsive to the referee's concern regarding the reliability of the static and rolling-window results across heterogeneous market regimes.

5.3. Results of the ML models

In this section, we describe the estimates obtained by considering the ML models described. The total, short, and long run dynamic connectedness, obtained based on a 200-days rolling-window QVAR model, serve as dependent variables to be explained by the lagged economic and financial indicators. We consider all the possible combinations of explanatory variables and report the best performing models based on RMSE. Tables 6 and 7 unveil the best performing models[2] relative to lower and upper quantiles and by considering the total dynamic connectedness.

In Table 6, the analysis highlighting the top 20 forecasting models (like for the lower quantile) provides a compelling perspective on the dynamics driving market behavior. The performance of these models is primarily measured by applying the most stringent measures to minimize the RMSE and maximize the coefficient of determination (R^2). The most promising model among these attains an RMSE of 1.02 and an R^2 of 33.5%. Three factors that have been strategically paired to create this

[2] The neural network architectures of the best fitting models are reported in the appendix. They serve as complementary materials reflecting the intrinsic linkages between the variables (inputs).

performance are the lagged VIX, which measures market volatility, the gold/Bitcoin ratio, indicative of investor sentiment and asset allocation preferences, and the Lagged Five-year inflation expectation (T5YIFR), a crucial indicator of future economic conditions. The addition of these factors to SVM produces highly accurate predictions that outperform other models, especially the XGBoost model in nine instances. Upon further scrutiny of the top 20 models, it becomes clear that the intrinsic mechanisms driving total connectedness in markets during stress periods are multifaceted and intricate. This discovery is hardly expected, as markets are often affected by sudden and intricate changes brought about by economic and geopolitical shocks. Consequently, the identification of these models and their root causes provide significant insights for investors, policymakers, and researchers who aim to navigate and forecast market trends with greater accuracy. In addition, the success of the SVM in this scenario emphasizes that machine learning techniques can be utilized to identify subtle patterns in financial data, which enables better predictive capabilities. By examining Table 7, the outcomes demonstrate that market trends can be predicted by selecting specific factors, emphasizing the multifaceted and fluctuating nature of market interdependence. This complex knowledge can assist in devising more robust investment strategies and policy interventions, enhancing the stability and effectiveness of financial markets.

Table 6. Best performing models, dependent variable TCI, τ=5%.

Method	Features	RMSE	R^2
SVM	diff_RATIO_lag1, T5YIFR_lag1, VIXCLS_lag1	1.020	0.335
SVM	diff_RATIO_lag1, diff_T10Y2Y_lag1, T5YIFR_lag1, VIXCLS_lag1	1.029	0.323
SVM	diff_BAMLC0A0CM_lag1, diff_RATIO_lag1, T5YIFR_lag1, VIXCLS_lag1	1.031	0.321
SVM	diff_BAMLC0A0CM_lag1, diff_RATIO_lag1, diff_T10Y2Y_lag1, T5YIFR_lag1, VIXCLS_lag1	1.043	0.305
SVM	T5YIFR_lag1, VIXCLS_lag1	1.058	0.284
SVM	diff_BAMLC0A0CM_lag1, T5YIFR_lag1, VIXCLS_lag1	1.064	0.277
SVM	diff_T10Y2Y_lag1, T5YIFR_lag1, VIXCLS_lag1	1.065	0.276
SVM	diff_BAMLC0A0CM_lag1, diff_T10Y2Y_lag1, T5YIFR_lag1, VIXCLS_lag1	1.074	0.263
SVM	diff_RATIO_lag1, VIXCLS_lag1	1.092	0.238
XGBoost	diff_RATIO_lag1, diff_T10Y2Y_lag1, T5YIFR_lag1, VIXCLS_lag1	1.096	0.232
SVM	diff_RATIO_lag1, diff_T10Y2Y_lag1, VIXCLS_lag1	1.097	0.231
XGBoost	diff_BAMLC0A0CM_lag1, diff_RATIO_lag1, diff_T10Y2Y_lag1, T5YIFR_lag1, VIXCLS_lag1	1.099	0.229
SVM	diff_BAMLC0A0CM_lag1, diff_RATIO_lag1, VIXCLS_lag1	1.100	0.226
SVM	diff_BAMLC0A0CM_lag1, diff_RATIO_lag1, diff_T10Y2Y_lag1, VIXCLS_lag1	1.108	0.215
XGBoost	diff_BAMLC0A0CM_lag1, T5YIFR_lag1, VIXCLS_lag1	1.116	0.204
XGBoost	diff_BAMLC0A0CM_lag1, diff_T10Y2Y_lag1, T5YIFR_lag1, VIXCLS_lag1	1.116	0.204
XGBoost	diff_BAMLC0A0CM_lag1, diff_RATIO_lag1, T5YIFR_lag1, VIXCLS_lag1	1.119	0.200
XGBoost	diff_T10Y2Y_lag1, T5YIFR_lag1, VIXCLS_lag1	1.124	0.193
XGBoost	diff_RATIO_lag1, T5YIFR_lag1, VIXCLS_lag1	1.127	0.189
SVM	VIXCLS_lag1	1.131	0.183

Table 7 demonstrates that the XGBoost algorithm is particularly effective in capturing market dynamics at upper quantiles, where it outperforms SVM, landing 18 out of the top 20 positions and attaining an RMSE of 1.14 and R^2 of 18.7%. These models, which are based on three key factors, the lagged differential maturity rate (T10Y2Y), gold/Bitcoin ratio, and ICE BofA Option-Adjusted Spread (OAS), are the high-performing specifications. They are most effective during challenging periods when volatility amplifies predictive signals. However, the accuracy is largely dependent on the gold/Bitcoin ratio as a constant, cross-quantile driver of precision, with only one factor considered universal in importance while the other factors are context-dependent. In tranquil market conditions, the heterogeneity of predictive patterns necessitates combinations of factors and differing model architectures, making adaptive modeling strategies a crucial consideration. The strength of XGBoost

in distilling intricate interdependencies from sparse inputs strengthens its advantage over SVM, particularly in scenarios that demand precision under uncertainty. Through its ability to adjust factor flexibility and algorithm efficiency to accommodate turbulent and tranquil regimes, XGBoost enhances forecast accuracy and becomes a useful tool for unraveling the intricate web of financial market connectivity.

Table 7. Best performing models, dependent variable TCI, τ=95%.

Method	Features	RMSE	R^2
XGBoost	diff_BAMLC0A0CM_lag1, diff_RATIO_lag1, diff_T10Y2Y_lag1	1.148	0.187
XGBoost	diff_RATIO_lag1, diff_T10Y2Y_lag1	1.154	0.178
XGBoost	diff_BAMLC0A0CM_lag1, diff_RATIO_lag1	1.157	0.175
XGBoost	diff_RATIO_lag1	1.158	0.172
XGBoost	diff_BAMLC0A0CM_lag1, diff_RATIO_lag1, diff_T10Y2Y_lag1, T5YIFR_lag1	1.171	0.155
XGBoost	diff_BAMLC0A0CM_lag1, diff_T10Y2Y_lag1	1.172	0.153
XGBoost	diff_RATIO_lag1, diff_T10Y2Y_lag1, T5YIFR_lag1	1.173	0.152
XGBoost	diff_T10Y2Y_lag1	1.174	0.150
XGBoost	diff_RATIO_lag1, diff_T10Y2Y_lag1, T5YIFR_lag1, VIXCLS_lag1	1.177	0.145
SVM	diff_BAMLC0A0CM_lag1, diff_RATIO_lag1, T5YIFR_lag1, VIXCLS_lag1	1.179	0.142
XGBoost	diff_RATIO_lag1, VIXCLS_lag1	1.179	0.142
XGBoost	diff_BAMLC0A0CM_lag1, diff_RATIO_lag1, diff_T10Y2Y_lag1, VIXCLS_lag1	1.181	0.140
XGBoost	diff_BAMLC0A0CM_lag1, diff_RATIO_lag1, T5YIFR_lag1	1.182	0.138
XGBoost	diff_BAMLC0A0CM_lag1, diff_RATIO_lag1, T5YIFR_lag1, VIXCLS_lag1	1.183	0.137
SVM	diff_RATIO_lag1, diff_T10Y2Y_lag1, T5YIFR_lag1, VIXCLS_lag1	1.185	0.134
XGBoost	diff_BAMLC0A0CM_lag1, diff_RATIO_lag1, diff_T10Y2Y_lag1, T5YIFR_lag1, VIXCLS_lag1	1.185	0.134
XGBoost	diff_BAMLC0A0CM_lag1	1.185	0.133
XGBoost	diff_BAMLC0A0CM_lag1, diff_RATIO_lag1, VIXCLS_lag1	1.186	0.133
XGBoost	diff_RATIO_lag1, T5YIFR_lag1	1.187	0.131
XGBoost	diff_RATIO_lag1, diff_T10Y2Y_lag1, VIXCLS_lag1	1.187	0.131

The predictive power of short-term dynamic connectedness, as depicted in Table 8 for the lower quantile, highlights the superiority of SVM in capturing crucial risk dynamics, which is consistent with its dominance in total connectedness metrics. Its top model's performance is largely due to its clever use of three critical elements, lagged VIX, in-depth knowledge of T10Y2Y interest rate differentials, and lagged five-year inflation expectations. Not only does this triumvirate of inputs reflect the interplay between macroeconomic tail risks, monetary policy changes, and inflationary pressures, but it also provides investors with a strong foundation to preemptively measure and mitigate downside risk exposure in adverse environments. Given that periods of elevated risk uncertainty are frequently accompanied by greater interdependence among asset classes and systemic vulnerabilities, the SVM model's ability to synthesize these delayed indicators into a precise forecast framework makes it an essential tool for proactive portfolio management. SVM's precision and its sensitivity to empirically verified risks enable market participants to shift from traditional risk monitoring paradigms and instead use a more proactive, data-driven approach. This enables them to navigate short term turbulence with greater resilience and strategic foresight.

Table 8. Best performing models, dependent variable Short, τ=5%.

Method	Features	RMSE	R^2
SVM	diff_T10Y2Y_lag1, T5YIFR_lag1, VIXCLS_lag1	12.241	0.067
SVM	T5YIFR_lag1, VIXCLS_lag1	12.245	0.066
SVM	diff_RATIO_lag1, T5YIFR_lag1, VIXCLS_lag1	12.252	0.065
SVM	diff_BAMLC0A0CM_lag1, diff_T10Y2Y_lag1, T5YIFR_lag1, VIXCLS_lag1	12.260	0.064
SVM	diff_BAMLC0A0CM_lag1, T5YIFR_lag1, VIXCLS_lag1	12.261	0.064
SVM	diff_RATIO_lag1, diff_T10Y2Y_lag1, T5YIFR_lag1, VIXCLS_lag1	12.272	0.062
SVM	diff_BAMLC0A0CM_lag1, diff_RATIO_lag1, T5YIFR_lag1, VIXCLS_lag1	12.280	0.061
SVM	diff_BAMLC0A0CM_lag1, diff_T10Y2Y_lag1, VIXCLS_lag1	12.281	0.060
SVM	diff_BAMLC0A0CM_lag1, VIXCLS_lag1	12.288	0.059
SVM	diff_BAMLC0A0CM_lag1, diff_RATIO_lag1, diff_T10Y2Y_lag1, VIXCLS_lag1	12.289	0.059
SVM	diff_BAMLC0A0CM_lag1, diff_RATIO_lag1, diff_T10Y2Y_lag1, T5YIFR_lag1, VIXCLS_lag1	12.289	0.059
SVM	diff_BAMLC0A0CM_lag1, diff_RATIO_lag1, VIXCLS_lag1	12.295	0.058
SVM	VIXCLS_lag1	12.353	0.049
SVM	diff_T10Y2Y_lag1, VIXCLS_lag1	12.362	0.048
SVM	diff_RATIO_lag1, VIXCLS_lag1	12.384	0.045
SVM	diff_RATIO_lag1, diff_T10Y2Y_lag1, VIXCLS_lag1	12.391	0.044
SVM	diff_T10Y2Y_lag1, T5YIFR_lag1	12.475	0.031
SVM	T5YIFR_lag1	12.490	0.028
XGBoost	diff_BAMLC0A0CM_lag1, T5YIFR_lag1	12.494	0.028
XGBoost	diff_BAMLC0A0CM_lag1, diff_T10Y2Y_lag1, T5YIFR_lag1	12.502	0.026

Table 9. Best performing models, dependent variable Short, τ=95%.

Method	Features	RMSE	R^2
SVM	diff_RATIO_lag1, VIXCLS_lag1	7.305	0.041
SVM	diff_BAMLC0A0CM_lag1, diff_RATIO_lag1, VIXCLS_lag1	7.341	0.031
SVM	diff_RATIO_lag1, T5YIFR_lag1, VIXCLS_lag1	7.353	0.028
SVM	T5YIFR_lag1, VIXCLS_lag1	7.375	0.022
SVM	diff_RATIO_lag1, diff_T10Y2Y_lag1, VIXCLS_lag1	7.378	0.022
SVM	diff_BAMLC0A0CM_lag1, T5YIFR_lag1, VIXCLS_lag1	7.378	0.021
SVM	VIXCLS_lag1	7.391	0.018
SVM	diff_BAMLC0A0CM_lag1, diff_RATIO_lag1, diff_T10Y2Y_lag1, VIXCLS_lag1	7.401	0.015
SVM	diff_BAMLC0A0CM_lag1, diff_RATIO_lag1, T5YIFR_lag1, VIXCLS_lag1	7.424	0.009
SVM	diff_BAMLC0A0CM_lag1, diff_RATIO_lag1, diff_T10Y2Y_lag1, T5YIFR_lag1, VIXCLS_lag1	7.425	0.009
SVM	diff_RATIO_lag1, diff_T10Y2Y_lag1, T5YIFR_lag1, VIXCLS_lag1	7.432	0.007
SVM	diff_T10Y2Y_lag1, VIXCLS_lag1	7.443	0.004
SVM	diff_BAMLC0A0CM_lag1, diff_T10Y2Y_lag1, T5YIFR_lag1, VIXCLS_lag1	7.450	0.002
SVM	diff_T10Y2Y_lag1, T5YIFR_lag1, VIXCLS_lag1	7.452	0.002
SVM	diff_BAMLC0A0CM_lag1, VIXCLS_lag1	7.461	-0.001
XGBoost	diff_BAMLC0A0CM_lag1, diff_RATIO_lag1, T5YIFR_lag1, VIXCLS_lag1	7.466	-0.002
XGBoost	diff_BAMLC0A0CM_lag1, T5YIFR_lag1, VIXCLS_lag1	7.467	-0.002
SVM	diff_BAMLC0A0CM_lag1, diff_T10Y2Y_lag1, VIXCLS_lag1	7.475	-0.004
XGBoost	diff_BAMLC0A0CM_lag1, diff_RATIO_lag1, T5YIFR_lag1	7.477	-0.005
SVM	T5YIFR_lag1	7.489	-0.008

SVM consistently outperforms its peers, as demonstrated by the empirical evidence presented in Table 9. The most significant and persuasive outcome of this examination is the revelation of a superior model that cleverly merges two crucial elements, the gold/Bitcoin ratio and the VIX, to produce optimal forecasting values. This is particularly noteworthy, as it shows that the gold/Bitcoin ratio and the VIX can be an extremely effective measure of dynamic connectedness, especially during times of market success (as evidenced by the upper quantile). Additionally, the analysis of the total dynamic connectedness shows that the predictive importance of these primary factors is not as significant but rather decreases due to lower R^2 and higher RMSE values. The divergence accentuates the intricacies and subtleties of the connections in question, necessitating a more detailed comprehension of how these variables are interrelated. Additionally, in the final analysis, our findings of this study hold significant importance for investors, policymakers, and market analysts, as they highlight the

significance of the gold/Bitcoin ratio and the VIX as indicators of market sentiment and dynamic connectivity, particularly during times of economic upheaval or prosperity. The information provided can aid stakeholders in devising better and wiser decisions, enabling greater market flexibility and precision, which helps minimize risks and maximize profits. The evidence presented in Table 9 provides a strong indication of the SVM model's ability to predict future outcomes while acknowledging the importance of the gold/Bitcoin ratio and the VIX as factors contributing to dynamic connectedness, emphasizing the need for broader market analysis and forecasting.

The predictive power of the SVM model is demonstrated in Tables 10 and 11, which highlight its ability to capture long-term financial connectivity during severe market conditions, a crucial aspect for investors who are cautious about risk exposure in uncertain circumstances. During times of systemic pressure, the SVM model is consistently more effective than other models, with indicators such as lagged VIX levels, maturity gap, and lagged ICE BofA spread being the most reliable. The top 20 models display differences in factor combinations, but their reliance on lagged indicators indicates a common trend: Market behavior is often driven by latent, interconnected dynamics during co-crash scenarios. The diversity emphasizes the importance of adaptive frameworks that accommodate changing risk pathways. Investing in long-term portfolios can be proactive in protecting against cascading crises by connecting them to these empirically proven drivers, transforming vulnerabilities into resilient, forward-looking opportunities. The validity of the outcomes obtained in stress situations lends credence to incorporating these indicators into portfolio construction, guaranteeing compliance with the ever-changing mechanics of systemic risk.

Table 10. Best performing models, dependent variable Long, τ=5%.

Method	Features	RMSE	R^2
SVM	diff_BAMLC0A0CM_lag1, diff_T10Y2Y_lag1, VIXCLS_lag1	12.753	0.060
SVM	diff_BAMLC0A0CM_lag1, VIXCLS_lag1	12.759	0.059
SVM	diff_BAMLC0A0CM_lag1, diff_RATIO_lag1, diff_T10Y2Y_lag1, VIXCLS_lag1	12.759	0.059
SVM	diff_BAMLC0A0CM_lag1, diff_RATIO_lag1, VIXCLS_lag1	12.759	0.059
SVM	diff_RATIO_lag1, diff_T10Y2Y_lag1, VIXCLS_lag1	12.760	0.058
SVM	diff_T10Y2Y_lag1, T5YIFR_lag1, VIXCLS_lag1	12.766	0.058
SVM	diff_RATIO_lag1, T5YIFR_lag1, VIXCLS_lag1	12.768	0.057
SVM	T5YIFR_lag1, VIXCLS_lag1	12.775	0.056
SVM	diff_BAMLC0A0CM_lag1, diff_T10Y2Y_lag1, T5YIFR_lag1, VIXCLS_lag1	12.775	0.056
SVM	diff_RATIO_lag1, diff_T10Y2Y_lag1, T5YIFR_lag1, VIXCLS_lag1	12.775	0.056
SVM	diff_BAMLC0A0CM_lag1, T5YIFR_lag1, VIXCLS_lag1	12.791	0.054
SVM	diff_BAMLC0A0CM_lag1, diff_RATIO_lag1, T5YIFR_lag1, VIXCLS_lag1	12.791	0.054
SVM	diff_BAMLC0A0CM_lag1, diff_RATIO_lag1, diff_T10Y2Y_lag1, T5YIFR_lag1, VIXCLS_lag1	12.792	0.054
SVM	diff_RATIO_lag1, VIXCLS_lag1	12.844	0.046
SVM	T5YIFR_lag1	12.871	0.042
SVM	diff_BAMLC0A0CM_lag1, T5YIFR_lag1	12.887	0.040
SVM	diff_T10Y2Y_lag1, T5YIFR_lag1	12.888	0.040
SVM	diff_RATIO_lag1, T5YIFR_lag1	12.903	0.037
SVM	diff_BAMLC0A0CM_lag1, diff_T10Y2Y_lag1, T5YIFR_lag1	12.906	0.037
SVM	diff_BAMLC0A0CM_lag1, diff_RATIO_lag1, T5YIFR_lag1	12.922	0.034

Even during periods of market distress, the SVM model exhibits an ability to maintain a comparatively better performance in predicting long-run dynamic connections, which is superior to what the XGBoost offers. A significant finding is that, even at low volatility levels, the SVM model is better suited to dealing with the complex dynamics of markets. Furthermore, the study suggests that lagged gold/Bitcoin ratio and lagged VIX provide together the best long-run prediction power, thus giving investors valuable information for maximizing expected gains. By utilizing these metrics,

investors can make informed investment choices and prepare for potential market fluctuations, which will yield higher returns. The implications are significant, as it signifies that investors can utilize the predictive capabilities of the SVM model, along with the lagged gold/Bitcoin ratio and VIX, to navigate the markets with greater confidence and precision. The outcome can be improved portfolio management, risk reduction, and increased profitability. Hence, investors must be aware of the potential of this model and these key metrics and accordingly incorporate them into their investment plans, especially during periods of market stability. By doing so, investors can stay ahead of the curve and capitalize on new opportunities, even in markets that are notorious for volatility. The ability to predict market movements with greater precision is a desirable attribute, and the SVM model, along with the lagged gold/Bitcoin ratio and VIX, provides optimum efficiency for this purpose, making it an essential tool for any investor. The outcomes highlight the need of utilizing data to guide investment, using machine learning and predictive analytics to enhance decision-making. This approach enables investors to invest in their portfolios, minimize risk, and capitalize on emerging trends, ensuring long-term success in an increasingly complex and interdependent global market.

Table 11. Best performing models, dependent variable Long, τ=95%.

Method	Features	RMSE	R^2
SVM	diff_RATIO_lag1, VIXCLS_lag1	7.577	0.066
SVM	diff_RATIO_lag1, T5YIFR_lag1, VIXCLS_lag1	7.586	0.064
SVM	diff_BAMLC0A0CM_lag1, diff_RATIO_lag1, VIXCLS_lag1	7.605	0.059
SVM	diff_BAMLC0A0CM_lag1, diff_RATIO_lag1, T5YIFR_lag1, VIXCLS_lag1	7.611	0.058
SVM	diff_BAMLC0A0CM_lag1, T5YIFR_lag1, VIXCLS_lag1	7.616	0.056
SVM	diff_RATIO_lag1, diff_T10Y2Y_lag1, VIXCLS_lag1	7.629	0.053
XGBoost	diff_BAMLC0A0CM_lag1, diff_RATIO_lag1, T5YIFR_lag1, VIXCLS_lag1	7.646	0.049
SVM	T5YIFR_lag1, VIXCLS_lag1	7.647	0.049
SVM	diff_BAMLC0A0CM_lag1, diff_RATIO_lag1, diff_T10Y2Y_lag1, T5YIFR_lag1, VIXCLS_lag1	7.660	0.045
SVM	diff_BAMLC0A0CM_lag1, diff_RATIO_lag1, diff_T10Y2Y_lag1, VIXCLS_lag1	7.661	0.045
XGBoost	diff_BAMLC0A0CM_lag1, diff_RATIO_lag1, diff_T10Y2Y_lag1, T5YIFR_lag1, VIXCLS_lag1	7.671	0.043
SVM	T5YIFR_lag1	7.672	0.043
SVM	diff_RATIO_lag1, diff_T10Y2Y_lag1, T5YIFR_lag1, VIXCLS_lag1	7.675	0.042
SVM	diff_BAMLC0A0CM_lag1, VIXCLS_lag1	7.675	0.042
SVM	diff_BAMLC0A0CM_lag1, diff_T10Y2Y_lag1, T5YIFR_lag1, VIXCLS_lag1	7.681	0.040
SVM	VIXCLS_lag1	7.694	0.037
SVM	diff_T10Y2Y_lag1, T5YIFR_lag1, VIXCLS_lag1	7.702	0.035
SVM	diff_RATIO_lag1, T5YIFR_lag1	7.709	0.033
XGBoost	diff_BAMLC0A0CM_lag1, diff_RATIO_lag1, VIXCLS_lag1	7.711	0.033
SVM	diff_BAMLC0A0CM_lag1, diff_RATIO_lag1, diff_T10Y2Y_lag1, T5YIFR_lag1	7.716	0.032

To further assess the crucial role that could be played by the factors considered, more profound investigations are conducted based on the importance plots and Shapley values. This analysis focuses on the lower quantile (τ =5%), given its greater relevance for systemic risk and tail-event forecasting.

Figure 3 underscores the nuanced yet critical roles of explanatory factors in predicting the dynamic 5% quantile connectedness between green bonds and US high-tech stocks, with the SVM and XGBoost models revealing striking consistencies and divergent insights. For the SVM model, the VIX index emerges as the unequivocal linchpin across short- and long-term horizons, dominating as the primary driver due to its influence during periods of market stress. Complementing this, the five-year expected inflation rate and the gold/Bitcoin ratio follow as secondary determinants, with the former commanding significance in the short term and the latter particularly in the long run and total connectedness metrics. Conversely, the XGBoost model aligns closely with SVM in the short term but reveals a compelling shift in the long run, where the five-year expected inflation rate surges to

prominence, not only outpacing the gold/Bitcoin ratio but also anchoring the total connectedness dynamics. These findings demonstrate that the predictive weight of variables is neither static nor uniform; instead, they vary dramatically across models and timeframes, necessitating a model-specific, context-sensitive approach to forecasting. By illuminating such heterogeneity, the analysis not only validates the robustness of machine learning in capturing extreme market dependencies but also advocates for a diversified toolkit to navigate the complexities of asset interlinkages during turbulent episodes, where traditional indicators may falter and alternative metrics rise to prominence.

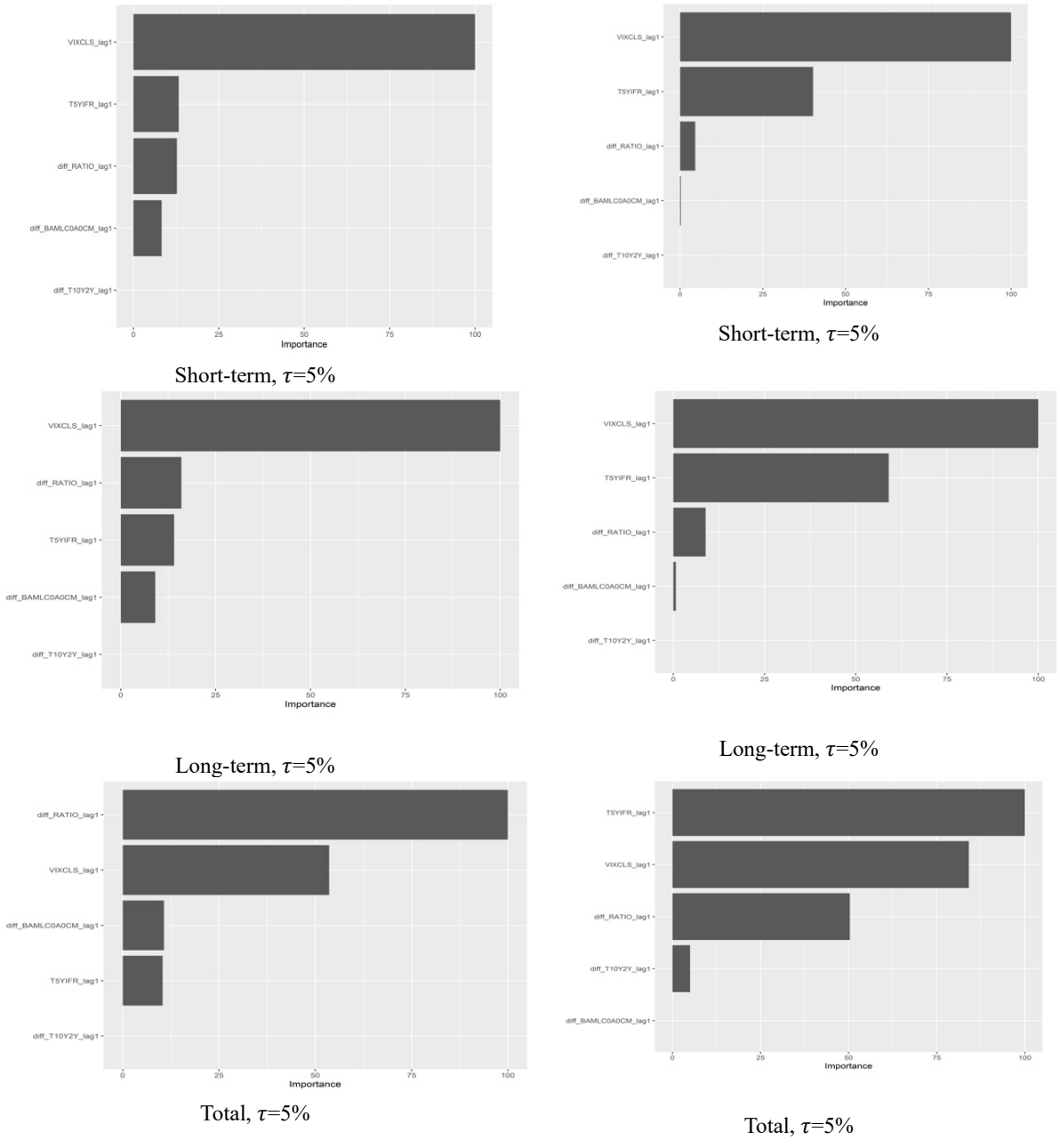


Figure 3. Feature Importance Plots for SVM (left) and XGBoost (right), lower quantile (τ=5%).

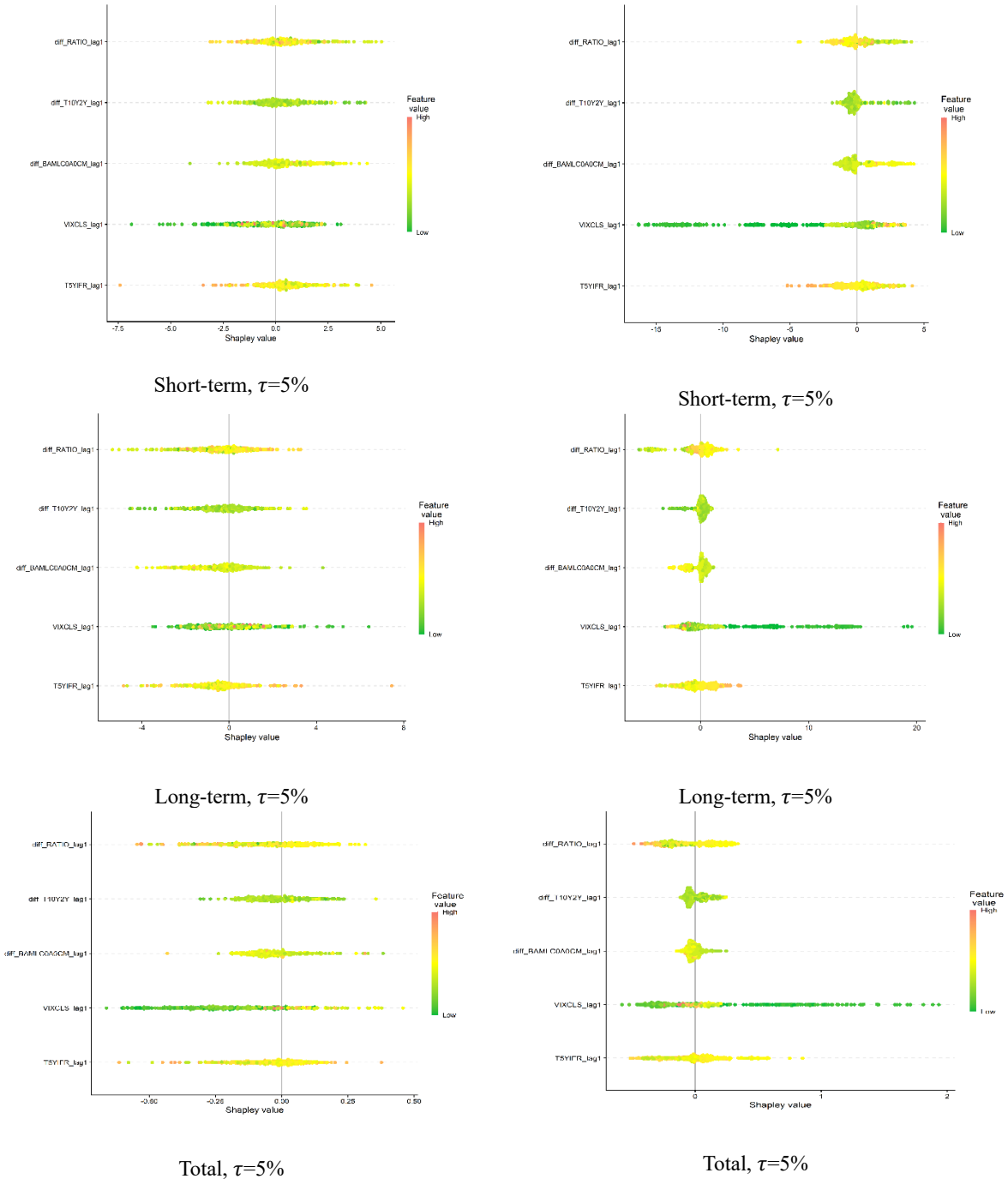


Figure 4. Shapley plots for SVM (left) and XGBoost (right), lower quantile (τ=5%).

The SHapley Additive (SHAP) value plots in Figure 4 provide a clear and actionable view of how individual predictors affect the models' connectedness forecasts. In these beeswarm plots, each point represents an observation, with the horizontal axis measuring the SHAP value, that is, the marginal contribution of the feature to the predicted TCI relative to its baseline level, and the color scale indicating the underlying feature magnitude. Positive SHAP values imply that a given realization of the predictor raises the forecasted connectedness, whereas negative values imply a downward

contribution. This representation helps to demystify model behavior and enables practitioners to identify which variables most consistently drive increases or decreases in predicted connectedness across explanatory variables and forecast horizons at the lower quantile (τ=5%).

According to Figure 4, VIX has the widest horizontal spread, indicating its largest average magnitude of SHAP values regardless of the short-term, long-term, and total connectedness. The other factors are marked by a narrower spread thus having an overall smaller impact on the predictions. More importantly, the graphs underscore that high VIX values (green/yellow) lead to extreme negative values, pushing predicted dynamic connectedness downward. The XGBoost model shows a different feature since the VIX is the most influencing factor leading to the highest rates (green) pointing on the left (negative SHAP value) in the short term but also scattered on the right implying a positive influence over the long term and for the total connectedness. This is indicative of a switch from a negative influence in the short run to a positive impact over the long run as VIX tends to either push the overall connectedness to plunge or to sharply increase during bearish markets conditions. The remaining factors have relatively small predictive impacts.

6. Discussion

In this section, we situate the empirical evidence from the static and time-varying FQVAR models, together with the machine learning results, within the broader literature on green bond and technology-asset connectedness and draw out its implications for sustainable finance.

Across the static and time-varying specifications, green bonds consistently emerge as the dominant net receiver of shocks in the system, remaining structurally insulated from the tech and AI/cybersecurity cluster at the aggregate level. This is consistent with evidence that green bonds act as resilient shock absorbers relative to conventional and emerging asset classes during periods of market stress (Xu et al., 2024), and with findings that connectedness between green bonds and equity markets intensifies during crises without green bonds becoming a primary spillover source (Mensi et al., 2022). Our frequency decomposition adds an important qualification to this picture, however: Green bonds' insulation is a short-term phenomenon that becomes markedly less pronounced once the horizon lengthens. This is in line with Pham and Nguyen (2021), who documented that the tail dependence between green bonds and other asset classes is asymmetric and concentrated around extreme market movements rather than uniform across the return distribution, and with Huynh et al. (2020), who found heavy-tail dependence between AI-related equities, green bonds, and cryptocurrencies that intensifies during periods of economic turbulence. AI/cybersecurity ETFs (BOTZ, CIBR) and mega-cap technology stocks (MSFT, NVDA) are identified as consistent net transmitters in our system, reinforcing evidence that technology and FinTech-adjacent assets are a source, rather than a recipient, of risk spillovers to green assets (Urom, 2023).

The TVP-FQVAR extension (Section 3.1.1) contributes a further, more specific finding to this literature. While the aggregate Total Connectedness Index is remarkably stable whether static or time-varying parameters are assumed (Section 5.2), the identity of the dominant net transmitters is not: Under time variation, NVDA and TSLA emerge as the strongest net transmitters in the system at the lower quantile (τ=5%), a role they do not occupy under the static model. This reallocation of directional risk is concentrated in the lower-tail, distress regime, while the upper-quantile (τ=95%) directional structure remains close to the static estimates. This asymmetry is a novel contribution relative to related time-varying connectedness studies: Abdelmalek and Khemakhem (2025), applying

a TVP-VAR extended joint connectedness approach to green bonds and financial markets, similarly found that connectedness is highly time-varying and intensifies sharply during crisis periods, with the VIX emerging as its primary driver; our results extend this logic by showing that it is the directional structure of connectedness, rather than only its magnitude, that is unstable during distress. Kang et al. (2026), examining the ‘‘Magnificent Seven” technology stocks with a TVP-VAR frequency framework, similarly reported that shifts in US mega-cap technology connectedness are concentrated in short-horizon dynamics rather than longer-run structural change; consistent with our finding that short-term spillovers dominate total connectedness in this system, and that apparent “long-run” integration is better understood as a sequence of short-lived, regime-driven transmission episodes than as genuine structural convergence.

The machine learning results add a complementary, predictive dimension to these findings. Consistent with Abdelmalek and Khemakhem (2025), who identified the VIX as a key driver of green bond connectedness during crises, implied that equity volatility is among the most consistently selected predictors of connectedness in our SVM and XGBoost models (Section 5.3). The gold-to-Bitcoin ratio also emerges as a robust predictor across specifications, a result that, to our knowledge, has not been documented in this literature; we interpret this as capturing the relative risk appetite between a traditional safe haven and a speculative digital asset, with shifts in this ratio proxying for liquidity-driven reallocations that transmit into the green bond-tech equity system independently of VIX-based volatility risk. The extension reported in Appendix B, in which the macro-financial predictor set is replaced with uncertainty and sentiment-based indicators (EPU, ADS, GPR, and MCCC), further refines this picture: The expanded predictor set underperforms the macro-financial specification at the lower quantile across all three connectedness measures, but is competitive with, and in two cases marginally exceeds, the macro-financial specification at the upper quantile. Within this expanded set, predictive power is driven overwhelmingly by the ADS Business Conditions Index rather than by the purely sentiment-based indicators, suggesting that observable real-economy conditions, rather than textual measures of uncertainty per se, carry the more useful signal for forecasting connectedness. Taken together, these results indicate that connectedness during market distress is better explained by market-based risk and liquidity signals than by broader policy or sentiment uncertainty, whereas the distinction between these predictor families narrows considerably away from the tail.

These findings carry direct implications for sustainable finance practice. Green bonds’ short-term vulnerability to shocks originating in AI and technology equities is a relevant consideration for ESG portfolio construction: A sharp technology-sector correction can transmit a temporary liquidity shock to green fixed income precisely when the cost of capital for climate-related projects is most sensitive to market conditions, even though green bonds’ longer-run structural role as a diversifier is not thereby undermined. This motivates a regime-aware approach to hedging rather than a static buy-and-hold ESG allocation: Our results suggest that periods of low implied volatility and a stable gold-to-Bitcoin ratio are associated with limited cross-asset spillover, whereas rising VIX or shifting risk-appetite signals coincide with a materially different connectedness structure in which technology equities, and specifically AI-related names, become more influential transmitters of shock to the green bond market.

Finally, in response to the referee’s suggestion that the quantile-based findings of this paper are connected explicitly to the Efficient Market Hypothesis (EMH), it is useful to first be precise about how our approach relates to the Quantile-on-Quantile (QQ) methodology of Sim and Zhou (2015). The QQ approach is a bivariate technique that estimates, via local linear regression, how a specific quantile of one variable responds to a specific quantile of another, thereby mapping the full dependence

structure between two series across their joint distribution rather than only at the conditional mean. Our TVP-FQVAR framework is not a QQ regression in this strict bivariate sense; however, it is built on the same underlying logic, generalized to a multivariate, network setting. The quantile vector autoregression that underlies our static and time-varying connectedness measures (Ando et al., 2022; Chatziantoniou et al., 2022) estimates system-wide relationships conditional on a specific quantile τ of the joint return distribution, and our frequency decomposition further conditions these relationships on the investment horizon. In this sense, our results can be read as a network-level, dynamic analogue of the QQ approach: Rather than mapping the pairwise dependence between two series across quantile pairs, we map how the system's connectedness structure, who transmits, who receives, and over what horizon, shifts across the quantiles of the joint distribution and, via the TVP-FQVAR, across time. A natural extension of this analysis, which we leave for future work, would complement this network-based view with bivariate QQ regressions between green bonds and specific technology assets, which would enable the local, pairwise dependence structure identified here to be mapped with the finer resolution the QQ method affords.

This quantile-conditional structure speaks directly to the question of market efficiency. The classical Efficient Market Hypothesis (Fama, 1970) posits that asset prices fully and continuously reflect available information, implying that the propagation of shocks between assets should be stable and largely independent of prevailing market conditions. Our results are difficult to reconcile with this description in its strict form: Connectedness in our system is low and comparatively stable around the median of the distribution, consistent with green bonds and technology equities being priced largely according to their own fundamentals under typical conditions, but rises sharply and becomes structurally different in the tails, where the TVP-FQVAR further reveals that even the identity of the dominant risk transmitters is unstable through time. This pattern of quantile- and regime-dependent efficiency is better described by the Adaptive Markets Hypothesis (AMH) of Lo (2004), which reframes market efficiency not as a fixed, binary property but as one that varies with prevailing market conditions as participants' behavior adapts to a changing environment. This regime-dependent view of efficiency is also found in the AI-token literature. For instance, Ko and Chen (2025), applying rescaled-range and wavelet coherence analysis to seven major AI tokens and Bitcoin, rejected the weak-form EMH in favor of the related Fractal Market Hypothesis and documented that AI-token/Bitcoin coherence varies across time and frequency, limiting Bitcoin's effectiveness as a hedge for this asset class. The result, in a purely digital-asset setting, resembles our own finding that cross-asset connectedness, and the identity of its dominant transmitters, is regime-dependent rather than constant. Under this reading, the near-decoupling of green bonds from technology equities during normal market conditions reflects a locally efficient market in Fama's sense, while the sharp, asymmetric, and–per our TVP-FQVAR results–time-varying increase in connectedness during periods of stress reflects the kind of state-dependent breakdown in efficiency that the AMH anticipates, consistent with related evidence that connectedness and market efficiency co-vary with prevailing conditions rather than remaining constant (Lo, 2004). Interpreted this way, our quantile- and frequency-based results provide empirical content for evaluating market efficiency conditionally on market regime and investment horizon, rather than treating efficiency as a single, sample-wide property of the green bond-technology equity system, and they suggest that risk management frameworks premised on constant, EMH-consistent cross-asset relationships are most likely to fail precisely in the tail states we identify as the least stable.

7. Conclusions

Green bonds, technology equities, and AI/cybersecurity ETFs exhibit significant regime-dependent and time–varying effects in their relationships. Green bonds are often viewed as diversification strategies but their compatibility with high-growth assets fluctuates, especially during market stressors. The asymmetric nature of financial connectedness is highlighted by the observation that spillover intensities are more significant at market extremes in both quantitative and frequency domain studies (Reboredo 2018). Training ML models on relevant macro-financial variables not only enhances spillover forecasting but also identifies the most potent contributors to systemic risk. SVM and XGBoost are superior to traditional neural networks in forecasting spillover dynamics at both tail quantiles, making them ideal for risk management in turbulent environments. A thorough understanding of the multi-horizon and non-linear spillover effects between green bonds, US technology stocks and AI/cybersecurity ETFs is necessary in today's interconnected financial landscape with complex trading patterns. By utilizing the FQVAR approach and contemporary machine learning techniques, researchers and practitioners can gain a deeper understanding of how shocks spread and what moderating factors contribute to financial connectedness. This integrated approach has the potential to enhance portfolio diversification, systemic risk measurement, and the formulation of resilient macroprudential policies.

Author contributions

Sami Mejri: Conceptualization; Writing–original draft; Writing–review & editing; Supervision; Project administration.

Arturo Leccadito: Methodology; Investigation; Formal analysis; Data curation; Visualization.

All authors have read and approved the final version of the manuscript.

Use of AI tools declaration

The authors declare they have not used Artificial Intelligence (AI) tools in the creation of this article.

Conflict of interest

The authors declare no conflict of interest.

References

Abdelmalek W, Khemakhem M (2025) Exploring the connectedness between green bonds and financial markets and its drivers during recent crises: New evidence from a TVP-VAR extended joint connectedness approach and wavelet coherence analysis. *Int J Financ Econ* 31: 2160-2179. https://doi.org/10.1002/ijfe.70035

Ando T, Greenwood-Nimmo M, Shin Y (2022) Quantile connectedness: Modeling tail behavior in the topology of financial networks. *Manage Sci* 68: 2401–2431. https://doi.org/10.1287/mnsc.2021.3984

Antonakakis N, Chatziantoniou I, Gabauer D (2020) Refined measures of dynamic connectedness based on time-varying parameter vector autoregressions. *J Risk Financ Manag* 13: 84. https://doi.org/10.3390/jrfm13040084

Ardia D, Bluteau K, Boudt K, et al. (2023) Climate change concerns and the performance of green vs. Brown stocks. *Manage Sci* 69: 7607–7632. https://doi.org/10.1287/mnsc.2022.4636

Aruoba SB, Diebold FX, Scotti C (2009) Real-time measurement of business conditions. *J Bus Econ Stat* 27: 417–427. https://doi.org/10.1198/jbes.2009.07205

Baker SR, Bloom N, Davis SJ (2016) Measuring economic policy uncertainty. *Q J Econ* 131: 1593–1636. https://doi.org/10.1093/qje/qjw024

Baruník J, Křehlík T (2018) Measuring the frequency dynamics of financial connectedness and systemic risk. *J Financ Econom* 16: 271–296. https://doi.org/10.1093/jjfinec/nby001

Caldara D, Iacoviello M (2022) Measuring geopolitical risk. *Am Econ Rev* 112: 1194–1225. https://doi.org/10.1257/aer.20191823

Chatziantoniou I, Abakah EJA, Gabauer D, et al. (2022) Quantile time–frequency price connectedness between green bond, green equity, sustainable investments and clean energy markets. *J Clean Prod* 361: 132088. https://doi.org/10.1016/j.jclepro.2022.132088

Chen KS (2024) Interlinkages between Bitcoin, green financial assets, oil, and emerging stock markets. *Data Sci Finance Econ* 4: 160–187. https://doi.org/10.3934/dsfe.2024006

Diebold FX, Yilmaz K (2008) Measuring financial asset return and volatility spillovers, with application to global equity markets. *Econ J* 119: 158–171. https://doi.org/10.1111/j.1468-0297.2008.02208.x

Diebold FX, Yilmaz K (2012) Better to give than to receive: Predictive directional measurement of volatility spillovers. *Int J Forecast* 28: 57–66. https://doi.org/10.1016/j.ijforecast.2011.02.006

Ehlers T, Packer F (2017) Green bond finance and certification. *BIS Quarterly Review*.

Estrella A, Mishkin F (1998) Predicting U.S. Recessions: Financial variables as leading indicators. *Rev Econ Stat* 80: 45–61. https://doi.org/10.1162/003465398557320

Fama EF (1970) Efficient capital markets: A review of theory and empirical work. *J Finance* 25: 383–417. https://doi.org/10.2307/2325486

Ferrer R, Shahzad SJH, Soriano P (2021) Are green bonds a different asset class? Evidence from time-frequency connectedness analysis. *J Clean Prod* 292: 125988. https://doi.org/10.1016/j.jclepro.2021.125988

Gilchrist S, Zakrajšek E (2012) Credit spreads and business cycle fluctuations. *Am Econ Rev* 102: 1692–1720. https://doi.org/10.1257/aer.102.4.1692

Hoang D, Wiegratz K (2023) Machine learning methods in finance: Recent applications and prospects. *Eur Financ Manag* 29: 1657–1701. https://doi.org/10.1111/eufm.12408

Huynh TLD, Hille E, Nasir MA (2020) Diversification in the age of the 4th industrial revolution: The role of artificial intelligence, green bonds and cryptocurrencies. *Technol Forecast Soc Change* 159: 120188. https://doi.org/10.1016/j.techfore.2020.120188

Kang H, Kwon M, Lee SG (2026) How the magnificent seven reshape market spillovers: TVP-VAR evidence. *Financ Res Lett* 101: 109942. https://doi.org/10.1016/j.frl.2026.109942

Ko PS, Chen KS (2025) Discovering AI tokens in the fractal markets hypothesis and their time-frequency co-movements with the leading high-carbon cryptocurrency. *Data Sci Finance Econ* 5: 293–319. https://doi.org/10.3934/dsfe.2025013

Koenker R, Bassett G (1978) Regression quantiles. *Econometrica* 46: 33. https://doi.org/10.2307/1913643

Konstantakis KN, Koulmas P, Michaelides PG, et al. (2025) Green bonds & clean energy in sustainable finance: Evidence from DCC-GARCH connectedness. *Int Rev Financ Anal* 103: 104168. https://doi.org/10.1016/j.irfa.2025.104168

Koop G, Korobilis D (2014) A new index of financial conditions. *Eur Econ Rev* 71: 101–116. https://doi.org/10.1016/j.euroecorev.2014.07.002

Lo AW (2004) The adaptive markets hypothesis: Market efficiency from an evolutionary perspective. *J Portf Manag* 30: 15–29. https://doi.org/10.3905/jpm.2004.442611

Mensi W, Shafiullah M, Vo XV, et al. (2022) Spillovers and connectedness between green bond and stock markets in bearish and bullish market scenarios. *Financ Res Lett* 49: 103120. https://doi.org/10.1016/j.frl.2022.103120

Naeem MA, Conlon T, Cotter J (2022) Green bonds and other assets: Evidence from extreme risk transmission. *J Environ Manage* 305: 114358. https://doi.org/10.1016/j.jenvman.2021.114358

Pham L, Nguyen CP (2021) Asymmetric tail dependence between green bonds and other asset classes. *Glob Financ J* 50: 100669. https://doi.org/10.1016/j.gfj.2021.100669

Reboredo JC (2018) Green bond and financial markets: Co-movement, diversification and price spillover effects. *Energy Econ* 74: 38–50. https://doi.org/10.1016/j.eneco.2018.05.030

Rundo F, Trenta F, Stallo AL di, et al. (2019) Machine learning for quantitative finance applications: A survey. *Appl Sci* 9: 5574. https://doi.org/10.3390/app9245574

Sim N, Zhou H (2015) Oil prices, US stock return, and the dependence between their quantiles. *J Bank Financ* 55: 1–8. https://doi.org/10.1016/j.jbankfin.2015.01.013

Tu Z, Yang R, Yang C (2024) Dynamics between FinTech and financial market: Supply-driven or demand-guided? *Quant Finance Econ* 8: 658–677. https://doi.org/10.3934/qfe.2024025.

Tunc A (2024) ETFs amidst the COVID-induced technological transformation: Sectoral insights from time-varying dynamics of tail risk transmissions. *N Am J Econ Financ* 74: 102243. https://doi.org/10.1016/j.najef.2024.102243

Urom C (2023) Time–frequency dependence and connectedness between financial technology and green assets. *Int Econ* 175: 139–157. https://doi.org/10.1016/j.inteco.2023.06.004

Wei P, Yuan K, Ren X, et al. (2023) Time-varying spillover networks of green bond and related financial markets. *Int Rev Econ Financ* 88: 298–317. https://doi.org/10.1016/j.iref.2023.06.022

Xu D, Hu Y, Corbet S, et al. (2024) Green bonds and traditional and emerging investments: Understanding connectedness during crises. *N Am J Econ Financ* 72: 102142. https://doi.org/10.1016/j.najef.2024.102142



AIMS Press

© 2026 the Author(s), licensee AIMS Press. This is an open access article distributed under the terms of the Creative Commons Attribution License (https://creativecommons.org/licenses/by/4.0)